6. Tightness of cask

It is verified that the activity leak rate L of the cask remains below the limit values valid according to traffic regulations for a type B(U) cask, both under normal operating conditions and under accidental conditions.

According to /6-1/, the admissible limits are:

Normal conditions:

$$L \cong 10^{-6} \cdot A_2/h$$

Accidental conditions:

$$L \cong 10^{-3} \cdot A_2/week$$

6.1 Initial data for verification

- The tightness system of the cask, which consists of three tightening points, has a leak rate of:

$$L_0 \cong 1.33 \cdot 10^{-4} \, bar \cdot cm^3 \, s^{-1} \, (\cong 10^{-4} \, Torr \cdot l \cdot s^{-1})$$

$$(L_0 \cong 3 \cdot 10^{-5} \, Torr \cdot l \cdot s^{-1} \, per \, gasket)$$

- Leak rates remain below this value, even under accidental conditions, as shown in drop tests.

- When preparing the cask for transport, an underpressure of 0.6 bar (related to temperature equilibrium) is established in the cask cavity, so as to create an inwards flowing gas stream.

- Fission gas inventory releases in MTR fuel assemblies (U-Al alloys) are negligible according to /6-2/ and /6-3/, as long as temperature remains below melting temperature.

Measurements carried out on the TN 7 cask loaded with 15 MERLIN and 45 DIDO fuel assemblies, of which some merely had the shortest cooling time permissible for transport, revealed no fission gases under operating conditions.

Although the melting temperature of the fuel assemblies is not reached, even in a fire, according to /6-4/, a release of 5 % of fission gases contained in the fuel assemblies is assumed under accidental conditions.

6.2 Verification methods

It is certified that under normal conditions underpressure inside the cask is maintained, so that no release of activity from the inside to the environment can occur.

Under accidental conditions, a release of 5 % of fission gases is assumed, based on /6-4/. It can however be verified that underpressure is maintained inside the cask even under accidental conditions.

6.3   Composition of fission gas

Only those nuclides are considered which are volatile at temperatures below the maximum fuel pin temperatures.

A. Loading with DIDO and MERLIN fuel assemblies

Calculation of the radioactive inventory was carried out in /6-5/. It will be presented briefly here.

The most unfavourable case of load is that of 60 DIDO fuel assemblies. The number of fissile U atoms in the cask then is:

$$No_{25} = \frac{60 \cdot 185 \cdot 6.02 \cdot 10^{23}}{235} = 2.84 \cdot 10^{25}$$

For a neutron flux of $\varnothing = 10^{14}$ n/sec $\cdot$ cm^2 (average flux) and a

period of irradiation $\tau = 6 \cdot 10^6$ sec,

one obtains according to /6-6/ the following fission gas inventory (stable and long lived radioactive isotopes):

Isotope	N_τ/No_{25}
Br 81	$7 \cdot 10^{-5}$
Kr 82	$5 \cdot 10^{-7}$
Kr 83	$1.5 \cdot 10^{-3}$
Kr 84	$4 \cdot 10^{-3}$
Kr 85	$1.1 \cdot 10^{-3}$
Kr 86	$7 \cdot 10^{-3}$
J 127	$6.5 \cdot 10^{-4}$
J 129	$3 \cdot 10^{-3}$
Xe 131	$8 \cdot 10^{-3}$
Xe 132	$1.5 \cdot 10^{-2}$
Xe 134	$2.5 \cdot 10^{-2}$
Xe 136	$4 \cdot 10^{-2}$
Sum	0.105

$\Sigma N_\tau = 0.105 \cdot 2.84 \cdot 10^{25} = 3.0 \cdot 10^{24}$ gas atoms in the fuel assemblies

B. RHF fuel assemblies

The fission gas inventory is determined as above according to /6-5/ and /6-6/.

$$No_{25} = \frac{2 \cdot 8556 \cdot 6.02 \cdot 10^{23}}{235} = 4.38 \cdot 10^{25} \text{ U-235 atoms}$$

For a neutron flux of $\varnothing = 1.5 \cdot 10^{14}$ n/sec $\cdot$ cm^2 (average flux) and a

period of irradiation $\tau = 44$ d $= 3.8 \cdot 10^6$ sec,

one obtains the following fission gas inventory (stable and long lived radioactive isotopes):

Isotope	N_τ/No_{25}
Br 81	$7 \cdot 10^{-5}$
Kr 82	$5 \cdot 10^{-7}$
Kr 83	$1.6 \cdot 10^{-3}$
Kr 84	$4 \cdot 10^{-3}$
Kr 85	$1.0 \cdot 10^{-3}$
Kr 86	$7.5 \cdot 10^{-3}$
J 127	$5.5 \cdot 10^{-4}$
J 129	$2.8 \cdot 10^{-3}$
Xe 131	$7 \cdot 10^{-3}$
Xe 132	$1.5 \cdot 10^{-2}$
Xe 134	$2.7 \cdot 10^{-2}$
Xe 136	$4.3 \cdot 10^{-2}$
Sum	0.109

$\Sigma N_\tau = 0.109 \cdot 4.38 \cdot 10^{25} = 4.77 \cdot 10^{24}$ gas atoms in the fuel assemblies

6.4   Tightness under normal conditions

With an assumed transport duration of t = 100 d (this is very conservative as in general transports last 20 days at the utmost), the pressure increase Δp is conservatively calculated in a simplified manner as follows:

$$\Delta p = \frac{L \cdot t}{V} = \frac{1.33 \cdot 10^{-4} \cdot 8.64 \cdot 10^{6}}{4.38 \cdot 10^{5}} = 2.6 \cdot 10^{-3} \text{ bar}$$

$V = 438 \, l = 4.38 \cdot 10^{5} \text{ cm}^3$ (minimum free cask volume)

$p_1 = p_0 + \Delta p = 0.6 \text{ bar} + 2.6 \cdot 10^{-3} \text{ bar}$

$p1 \approx = 0.6027$ bar = interior pressure in the cask after 100 d.

Pressure increases due to the leak rate of the tightening system during the considered 100 d is negligible.

According to conservative calculations, time required until pressure equilibrium is established is:

$$t = \frac{\Delta p \cdot V}{L} = -\frac{0.4 \cdot 4.38 \cdot 10^{5}}{1.33 \cdot 10^{-4}}$$

$t = 1.3 \cdot 10^{9}$ sec $\cong 41.8$ years

The gas flow is directed inward during a practically unlimited period of time, which means that no activity release occurs.

Before every transport, a leak rate of

$L \cong 1 \cdot 10^{-2}$ bar cm$^3 \cdot$ s^{-1}

is verified for the cask, so that maintenance of underpressure is assured within a transport period of 100 days.

$$\Delta p = \frac{1.10 \cdot 10^{-2} \cdot 8.64 \cdot 10^{6}}{4.38 \cdot 10^{5}} = 0.20 \text{ bar}$$

$p_1 = p_0 + \Delta p = 0.6 + 0.2 = 0.8 \text{ bar}$

6.5   Tightness under accidental conditions

It is assumed that 5 % of the fission gas inventory is released (according to /6-4/).

In case of fire, the average air temperature inside the cask increases by 150 K according to conservative estimates.

A. DIDO and MERLIN fuel assemblies

   - Pressure increase due to fission gases

   For a release of 5 %, the amount of gas atoms released into the cask is:

   $$Z = 0.05 \cdot 3.0 \cdot 10^{24} = 1.5 \cdot 10^{23}$$

   The resulting pressure increase Δp is:

   $$\Delta p = \frac{Z \cdot R \cdot T_0}{V \cdot L}$$

   with: $R = 8.315 \dfrac{J}{mole\,K}$ = general gas constant

   $L = 6.02 \quad 10^{23}$ 1/mole

   $V = 0.438\ m^3$

   $T_0 = 573\ K$ (average air temperature in the cask, conservative assumption)

   $\Delta p = 2.71 \cdot 10^3\ N/m^2 = 0.027$ bar ($\cong 20.3$ Torr)

Pressure inside the cask after release of fission gases:

$p_2 = p_1 + \Delta p = 0.6027 + 0.027 = 0.63$ bar

- Maximum pressure in the cask due to an accidental fire:

$$p_3 = \frac{T_1}{T_0} \cdot p_2$$

$$p_3 = \frac{723}{573} \cdot 0.63 = 0.80 \text{ bar}$$

The maximum expected interior pressure remains below ambient atmospheric pressure, so that no leak occurs.

B. RHF fuel assemblies

- Pressure increase due to fission gases

For a release of 5 %, the amount of gas atoms released into the cask is:

$$Z = 0.05 \cdot 4.77 \cdot 10^{24} = 2.385 \cdot 10^{23}$$

$$\Delta p = \frac{Z \cdot R \cdot T_0}{V \cdot L} = \frac{2.385 \cdot 10^{23} \cdot 8.135 \cdot 537}{0.509 \cdot 6.02 \cdot 10^{23}}$$

$$p = 3.63 \cdot 10^3 \text{ N/m}^2 = 0.0363 \text{ bar}$$

with: $T_0 = 573$ K = average air temperature in the cask according to conservative estimates

$$p_2 = p_1 + \Delta p = 0.6027 \cdot 0.0363$$

$$p_2 = 0.64 \text{ bar}$$

- Maximum pressure in the cask due to an accidental fire

$$p_3 = \frac{T_1}{T_0} \cdot p_2$$

$$= \frac{723}{573} \cdot 0.64 = 0.81 \text{ bar}$$

The maximum expected interior pressure remains below ambient atmospheric pressure, so that no leak occurs.

6.6   Literature

/6-1/   IAEA-Regulations for the Safe Transport of
           Radioactive Materials, 1973

/6-2/   M. B. Reynolds,
           Fission Gas Behaviour in the U-Al System,
           Nucl. Sc. and Eng., 3, 1958

/6-3/   H. W. Castleman et al.
           "Diffusion of Xe through Al and stainless steel",
           BNL 624, 1960

/6-4/   P. Rocco, IAEA-SR-10/43

/6-5/   TN 7/MTR Package Design, Safety Report,
           TN Report No. 7701

/6-6/   I. O. Blomeke/M. F. Todd
           U-235 Fission Product Production as a Function of
           Thermal Neutron Flux, Irradiation Time and Decay Time,
           ORNL 2127, Oak Ridge

7.   Dose rate at cask surface

It is demonstrated that under normal transport conditions and accidental conditions, the dose rate (DR) at the surface of the cask remains below the admissible limits according to traffic regulations based on IAEA Rules /7-7/:

Normal conditions:	surface	$DR \cong 200$ mrem/h
	2 m distance	$DR \cong 10$ mrem/h
Accidental conditions:	1 m distance	$DR \cong 1000$ mrem/h

7.1   Structure of shielding

Shielding thicknesses indicated below are maintained also after the testing conditions for type B casks, as already verified in chapter 4.5. The cement layer in the mantle dehydrates. Conservatively, the shielding effect of this layer under accidental conditions is negligible.

- Cask mantle
  (cf. Fig. 7-1)

Table 7-1: shielding thicknesses in the cask mantle

Material	Shielding thickness t (cm)	Density (g/cm³)
Steel	1.0	7.90
Lead	18.5	11.2
Cement	2.0 [1]	1.89
Steel	2.5	7.90

[1] Minimum thickness of the cement layer

- Shielding of the end surfaces
  (cf. Fig. 7-1)

Table 7-2: Shielding thicknesses on the lid end

Material	Shielding thickness t (cm)
Steel	1.0
Lead	16.5
Steel	7.0

Table 7-3: Shielding thicknesses on the bottom end

Material	Shielding thickness t (cm)
Steel	1.75 [1]
Lead	17.0
Steel	2.5

[1] Average thickness of the bottom

The shock absorbers are not included in the calculation of the shielding of the front end. These results are thus conservative.

7.2 Source intensities

The MTR fuel assemblies which are to be transported only have negligible neutron source intensities. Only gamma sources must be taken into account for shielding calculations.

A. DIDO and MERLIN fuel assemblies

According to /7-1/, the source intensity with a load of 4 DIDO insert baskets is identical to that with 3 DIDO and 1 MERLIN insert baskets, which means that in this case the same values may be expected. Gamma source intensities according to /7-1/ are taken, as the same conditions apply (cf. also chapter 2.5):

Power per fuel assembly: 1.0 $_{MWth}$/assembly
Irradiation period: $t_B = 70 \, d = 6 \cdot 10^6$ sec
Cooling time: $t_A = 231 \, d = 2 \cdot 10^7$ sec

The cooling time is averaged in such a way that thermal power per insert basket remains below 1125 W.

Source intensities were obtained from /7-2/.

Following source intensities are found:

Table 7-4a: Gamma source intensities of DIDO and MERLIN fuel assemblies

Energy group	Source intensity S/cask (1/sec)	Volume source intensity S_V (1/s · cm^3)
1 - 1.7 MeV (reference energy 1.5 MeV)	$1.32 \cdot 10^{14}$	$2.34 \cdot 10^8$
> 1.7 MeV (reference energy 2.0 MeV)	$5.28 \cdot 10^{13}$	$9.35 \cdot 10^7$

The volume source intensity of the fuel assemblies homogenised in the interior cask cavity is calculated according to:

$$S_v = \frac{S}{R_0^2 \cdot \pi \cdot h}$$

with: R_0 = 26 cm = radius of insert baskets

H = 266 cm = height of the four insert baskets

B. RHF fuel assemblies

The source intensities are taken from /7-3/, as the initial conditions for the fuel assemblies are the same.
Total source intensities were assessed according to /7-2/.

Power per fuel assembly: P = 0.25 MW$_{th}$/assembly

Irradiation time: t_B = 44 d = 3.8 $\cdot$ 10^6 sec

Cooling time: t_A = 310 d = 2.68 $\cdot$ 10^7 sec

The following source intensities result:

Table 7-4b: Gamma source intensities of RHF fuel assemblies

Energy group	Source intensity S/cask (1/sec)	Source intensity S of the linear source (1/sec)	Source intensity S_L per unit length (1/sec)
1 - 1.7 MeV (ref. energy 1.5 MeV)	1.28 $\cdot$ 10^{14}	8 $\cdot$ 10^{12}	3.96 $\cdot$ 10^{10}
> 1.7 MeV (ref. energy 2.0 MeV)	1.90 $\cdot$ 10^{13}	1.19 $\cdot$ 10^{13}	5.89 $\cdot$ 10^9

Homogeneous fuel distribution is assumed within the fuel assembly annulus. This annulus is subdivided into 16 linear sources (Fig. 7-2). The source intensity of the linear source is calculated according to:

$$S_L = \frac{S}{16 \cdot H}$$

with: H = 202 cm (height of the 2 fuel assemblies including the distance between them)

7.3   Calculation methodology

A. DIDO and MERLIN fuel assemblies

Calculation of dose rates at the mantle and the front ends is carried out applying Rockwell's volume source model /7-4/. Fuel assemblies and insert basket parts in the volume of cylinder sources are homogenised.

Calculation is carried out according to the following equations:

- Maximum dose rates at the mantle (central plane)

$$D = U \cdot \frac{B \cdot S_v}{4 \cdot (a+z)} \cdot F(\theta, b_2)$$

- Maximum dose rate at the front ends ("upper limit": $h \cong \frac{3}{\mu_s}$)

$$D = U \cdot \frac{B \cdot S_v}{2 \cdot \mu_s} \cdot \left[E_2(b) - \frac{E_2(b \cdot \sec \theta)}{\sec \theta} \right]$$

with: U   =   conversion factor for the assessment of the dose rate from the flux of gamma quanta
(mrem · h-1 · cm2 · sec)

B   =   build-up factor

S_v =   volume source intensity /1/s · cm^3)

$F(\theta, b_2)$ =   attenuation factor according to table in /7-4/

$\tan \theta$ = $\dfrac{H}{a+z}$ (mantle), $\tan \theta = \dfrac{R_0}{a}$ (front ends)

H   =   source height

a   =   distance between source and point of calculation

b   =   length of relaxation = $\Sigma \mu_i \cdot t_i$

b_2 = $b + \mu_s \cdot z$

μ_i	=	macroscopic cross-section of shielding element i (according to /7-5/)
t_i	=	thickness of shielding element i
z	=	thickness of source self-shielding according to /7-4/
μ_s	=	macroscopic cross-section of the source. The latter consists of the fuel assemblies and the corresponding parts of the insert baskets.

$$\mu_s = \left(\sum \frac{\mu_i}{d_i} \cdot \frac{A_i}{100} \right) \cdot d_s$$

A_i	=	% weight participation of fuel assembly i in the source
d_s	=	density of the homogenised source

$$E_2(b) - \frac{E_2(b \cdot \sec \theta)}{\sec \theta}$$ This expression is determined from graphs in /7-4/.

Values μ_s and μ_i/d_i are represented in tables further on.

B. RHF fuel assemblies

Calculation of dose rates at the mantle and the front ends is carried out similarly to /7-3/ according to Rockwell's linear source model, with source intensities determined in 7.2. Self-shielding in the linear sources is taken into account.

The calculation model permits:

- taking into account of the different distances between the single sources and the receiving point;

- taking into account of shielding thickness increase due to radiation traversing the cask walls askew.

Geometric conditions are described in fig. 7-3. The following equation applies:

- Maximum dose rate at the mantle (central plane)

$$D = U \cdot \frac{B \cdot S_{LS}}{2 \cdot \pi \cdot a} \cdot F(\theta_1, b_1) \text{ with } a = 1_3$$

- Maximum dose rate at the front ends ($h \cong \dfrac{3}{\mu_s}$)

$$D = U \cdot \frac{B \cdot S_{LS}}{4 \cdot \pi \cdot a} \cdot [F(\theta_1, b_1) - (F(\theta_2, b_2)]$$

$$S_{LS} = \frac{S_L}{\alpha} \cdot (1 - \frac{1}{e^\alpha})$$

with S_L according to chapter 7.2.

$\alpha = \mu_s \cdot a$ (μ_s according to table 7-5, a = 6.8 cm, cf. fig. 7-2),

the signification of every factor being the same as described under 7.3A. The effective b-value for the single linear sources at the mantle is determined according to the following method:

$$b_{eff} = b' \cdot \frac{1_2 - 1_1}{r_a - r_i}$$

with   b' = b for sources 1 - 8

           b' = b + t · μ_s for sources 9 - 16

           (b according to tables 7-6 till 7-8; μ_s according to table 7-5)

   t = 6.8 cm (cf. fig. 7-2)

The b_{eff} values, build-up factors and $F(\theta, b)$ values are listed in tables 7-10 and 7-11 for the single linear sources.

Only one side of the annulus is considered, for reasons of symmetry, that is linear sources 1 - 4 and 9 - 12. Total dose rate is then calculated from the sum of the single dose rates of the considered linear sources, multiplied by 2.

7.4   Initial data

7.4.1   Cross sections for gamma radiation

The values for macroscopic cross-sections μ (cm^{-1}) of shielding materials are determined based on the mass attenuating coefficients μ/ρ (cm^2/g) according to /7-5/.

The values μ/ρ, μ and b are represented in tables 7-6, 7-7 and 7-8.

7.4.2   Build-up factor

The values for build-up B are determined according to Broder's method /7-6/, p. 231.

7.4.3   Conversion factor

The conversion factor U to determine dose rates based on the flux is found in /7-6/ (cf. table 7-9).

Table 7-5: Macroscopic cross-section μ_S of the source

A. DIDO and MERLIN fuel assemblies

Energy group (MeV)	1,5	2,0
μ_{Fe}/ρ_{Fe}	0,0485	0,0424
μ_U/ρ_U	0,0548	0,0484
μ_{Al}/ρ_{Al}	0,0500	0,0432
μ_S	0,0596	0,0520

$\rho_S = 1,22$ g/cm³

The bottom plates of the insert baskets were neglected because they are not oriented in the direction of radiation.

The weight of the source is composed of:

- 60 fuel assemblies: 12 kg uranium
                                                        + 150 kg aluminum
                                                           162 kg
- 4 insert baskets: + 580 kg steel
                                                        -   54 kg steel (bottom plates)
                                                           688 kg

B. RHF fuel assemblies

Energy group (MeV)	1,5	2,0
μ_U/ρ_U	0,0548	0,0484
μ_{Al}/ρ_{Al}	0,0500	0,0432
μ_S/ρ_S	0,0504	0,0436
μ_S	0,0806	0,0698

$\rho_s = 1.6$ g/cm³
density of the homogenised annulus

Table 7-6: Cross sections, relaxation lengths and build-up factors for
dose rate calculation at the mantle

E-group	Material	Steel	Lead	Cement	b	B
	t (cm)	3,5	18,5	2,0		
1,5 MeV	μ/ρ (cm²/g)	0,0485	0,0512	0,0517		
	μ (cm^{-1})	0,3832	0,5734	0,0982	12,15	6,72
	$\mu \cdot t$ (-)	1,3410	10,6086	0,1965		
2,0 MeV	μ/ρ (cm²/g)	0,0424	0,0457	0,0445		
	μ (cm^{-1})	0,3350	0,5118	0,0846	10,81	5,73
	$\mu \cdot t$ (-)	1,1724	9,4690	0,1691		

Table 7-6: Cross sections, relaxation lengths and build-up factors for
dose rate calculation at the lid

E-group	Material	Steel	Lead	b	B
	t (cm)	8,0	16,5		
1,5 MeV	μ/ρ (cm²/g)	0,0485	0,0512		
	μ (cm^{-1})	0,3832	0,5734	12,53	7,36
	$\mu \cdot t$ (-)	3,0652	9,4618		
2,0 MeV	μ/ρ (cm²/g)	0,0424	0,0457		
	μ (cm^{-1}	0,3350	0,5118	11,13	6,34
	$\mu \cdot t$ (-)	2,6797	8,4454		

Table 7-8: Cross sections, relaxation lengths and build-up factors for dose rate calculation at the bottom

E-group	Material	Steel	Lead	b	B
	t (cm)	4,25	17,0		
1,5 MeV	μ/ϱ (cm²/g)	0,0485	0,0512		
	μ (cm^{-1})	0,3832	0,5734	11;38	6,25
	$\mu \cdot t$ (-)	1,6284	9,7485		
2,0 MeV	μ/ϱ (cm²/g)	0,0424	0,0457		
	μ (cm^{-1})	0,3350	0,5118	10,12	5,41
	$\mu \cdot t$ (-)	1,4236	8,7013		

Table 7-9: Conversion factor U for gamma radiation

E-group (MeV)	Reference energy (MeV)	Conversion factor $(mR \cdot h^{-1} \cdot s \cdot cm^2)$
1,5	1,5	$2,65 \cdot 10^{-3}$
2,0	2,0	$3,2 \cdot 10^{-3}$

Table 7-10: Initial data for dose rate calculations at the mantle surface (cask loaded with 2 RHF fuel assemblies)

Source Nr.	$l_2 - l_1$ (cm)	l_3 (cm)	θ	E-group (MeV)	b'	b_{eff}	B	$\Delta F(\theta,b)$
1	27,5	51,0	63,2	1,5	12,15	13,64	7,5	$3,88 \cdot 10^{-7}$
				2,0	10,81	12,13	6,4	$1,85 \cdot 10^{-6}$
2	27,3	44,4	66,3	1,5	12,15	13,54	7,5	$4,30 \cdot 10^{-7}$
				2,0	10,81	12,05	6,4	$2,01 \cdot 10^{-6}$
3	26,0	38,7	69,0	1,5	12,15	12,89	7,1	$8,42 \cdot 10^{-7}$
				2,0	10,81	11,47	6,1	$3,67 \cdot 10^{-6}$
4	24,7	35,2	70,8	1,5	12,15	12,25	6,8	$1,63 \cdot 10^{-6}$
				2,0	10,81	10,90	5,8	$6,65 \cdot 10^{-6}$
9	26,8	57,2	60,5	1,5	12,70	13,89	7,7	$2,99 \cdot 10^{-7}$
				2,0	11,28	12,34	6,5	$1,49 \cdot 10^{-6}$
10	25,8	62,4	58,3	1,5	12,70	13,37	7,4	$5,13 \cdot 10^{-7}$
				2,0	11,28	11,88	6,3	$2,40 \cdot 10^{-6}$
11	25,0	66,1	56,8	1,5	12,70	12,96	7,2	$7,83 \cdot 10^{-7}$
				2,0	11,28	11,51	6,1	$3,53 \cdot 10^{-6}$
12	24,6	68,0	56,0	1,5	12,70	12,75	7,0	$9,74 \cdot 10^{-7}$
				2,0	11,28	11,33	6,0	$4,25 \cdot 10^{-6}$

Table 7-11: Initial data for dose rate calculations at the mantle, at 2 m distance (cask loaded with 2 RHF fuel assemblies)

Source Nr.	l_2-l_1 (cm)	l_3 (cm)	θ	E-group (MeV)	b'	b_{eff}	B	$\Delta F(\theta,b)$
1	27,5	248,8	22,1	1,5	12,15	13,64	7,5	$3,39 \cdot 10^{-7}$
				2,0	10,81	12,13	6,4	$1,58 \cdot 10^{-6}$
2	26,6	242,6	22,6	1,5	12,15	13,19	7,3	$5,42 \cdot 10^{-7}$
				2,0	10,81	11,74	6,2	$2,38 \cdot 10^{-6}$
3	25,4	237,7	23,0	1,5	12,15	12,60	7,0	$9,97 \cdot 10^{-7}$
				2,0	10,81	11,21	5,9	$4,12 \cdot 10^{-6}$
4	24,6	235,1	23,2	1,5	12,15	12,20	6,7	$1,50 \cdot 10^{-6}$
				2,0	10,81	10,85	5,7	$5,98 \cdot 10^{-6}$
9	27,3	255,3	21,6	1,5	12,70	14,15	7,8	$2,0 \cdot 10^{-7}$
				2,0	11,28	12,57	6,7	$9,98 \cdot 10^{-7}$
10	26,3	261,2	21,1	1,5	12,70	13,63	7,5	$3,35 \cdot 10^{-7}$
				2,0	11,28	12,12	6,4	$1,56 \cdot 10^{-6}$
11	25,2	265,6	20,8	1,5	12,70	13,06	7,2	$5,94 \cdot 10^{-7}$
				2,0	11,28	11,60	6,1	$2,62 \cdot 10^{-6}$
12	24,6	268,0	20,6	1,5	12,70	12,75	7,0	$8,10 \cdot 10^{-7}$
				2,0	11,28	11,33	6,0	$3,44 \cdot 10^{-6}$

7.5 Calculation and results

7.5.1 Dose rates under normal transport conditions

7.5.1.1 Mantle dose rate

The maximum mantle dose rate is calculated for a point situated at the centre of the active zone. The active length was not subdivided into zones.

A. DIDO and MERLIN fuel assemblies

- Geometry for the calculation of the surface dose rate

$$H = 266 \text{ cm} = \text{height of source}$$

$$a = 25 \text{ cm} = \text{distance between source and point of calculation}$$

$$R_0 = 26 \text{ cm} = \text{radius of source}$$

$$\tan \theta = \frac{H/2}{a+z} = \frac{266/2}{25/z}$$

- Geometry for the calculation of the dose rate at a distance of 2 m

$$H = 266 \text{ cm} = \text{height of source}$$

$$a = 225 \text{ cm} = \text{distance between source and point of calculation}$$

$$R_0 = 26 \text{ cm} = \text{radius of source}$$

$$\tan \theta = \frac{H/2}{a+z} = \frac{266/2}{225/z}$$

The results of calculations are given below.

Table 7-12a: Mantle dose rate calculation for DIDO and
MERLIN fuel assemblies

Point of calculation at the cask	Surface		2 m distance	
E-group (MeV)	1,5	2,0	1,5	2,0
U (mrem$\cdot$h$^{-1}\cdot$sec$\cdot$cm²)	$2,65\cdot10^{-3}$	$3,2\cdot10^{-3}$	$2,65\cdot10^{-3}$	$3,2\cdot10^{-3}$
B	6,72	5,73	6,72	5,73
S_v (1/s$\cdot$cm³)	$2,34\cdot10^{8}$	$9,35\cdot10^{7}$	$2,34\cdot10^{8}$	$9,35\cdot10^{7}$
μ_S (cm^{-1})	0,0596	0,0520	0,0596	0,0520
b	12,15	10,81	12,15	10,81
Z (cm)	22,59	22,73	18,60	19,92
θ (°C)	70,31	70,26	28,66	28,53
b_2	13,49	11,99	13,17	11,78
ΔF (θ,b_2)	$4,35\cdot10^{-7}$	$2,14\cdot10^{-6}$	$6,02\cdot10^{-7}$	$2,51\cdot10^{-6}$
D (mrem/h)	13,1	25,5	3,5	5,9
D_{Ges} (mrem/h)	38,6		9,4	

B. RHF fuel assemblies

- Geometry for the calculation of the surface dose

H   =   202 cm   =   height of source

a   = l_3: cf. table 7-10 = distance between source and point of
                            calculation

U   : cf. table 7-9

B   : cf. table 7-10

F(θ, b)   : cf. table 7-10

S_{LS} = $S_L \cdot 0.77$ (1.5 MeV)
         = $S_L \cdot 0.796$ (2.0 MeV)

Table 7-12b: Dose rate at the mantle surface for 2 RHF
                fuel assemblies (mrem/h)

Source no.		1	2	3	4	9	10	11	12
D	1,5(MeV)	0,73	0,93	1,99	4,05	0,52	0,79	1,09	1,29
	2,0(MeV)	0,58	0,72	1,45	2,74	0,42	0,61	0,81	0,94
$D_1 = \Sigma D$		1,31	1,65	3,44	6,79	0,94	1,40	1,90	2,23

D_{Ges} = 2 $\cdot$ D_1 = 2 $\cdot$ 19,66

D_{Ges} = 39,3 mrem/h

- Geometry for the calculation of the dose rate at a distance of 2 m

a   = I_3: cf. table 7-11 = distance between source and point of calculation

U   : cf. table 7-9

B   : cf. table 7-11

F(θ, b)   : cf. table 7-11

S_{LS} =   cf. above

Table 7-12c: Mantle dose rate at 2 m distance for 2 RHF
              fuel assemblies (mrem/h)

Source no.		1	2	3	4	9	10	11	12
D	1,5(MeV)	0,13	0,21	0,38	0,55	0,08	0,12	0,21	0,27
	2,0(MeV)	0,10	0,15	0,25	0,37	0,06	0,10	0,15	0,19
D_1		0,23	0,36	0,63	0,92	0,14	0,22	0,36	0,46

$D_{Ges} = 2 \cdot D_1 = 2 \cdot 3,32$

$D_{Ges} = 6,6$ mrem/h

7.5.1.2 Dose rate at the lid

Dose rates are determined at the surface of the lid and at a distance of 2 m according to the equations in chapter 7.3. The active zone is considered as a total zone for calculations.

A. DIDO and MERLIN fuel assemblies

- Geometry for the calculation of dose rate at the surface

H = 266 cm = height of source

a = 24.5 cm = distance between source and point of calculation

R_0 = 26 cm = radius of source

$$\tan \theta = \frac{R_0}{a}$$

- Geometry for the calculation of dose rate at 2 m distance

H = 266 cm = height of source

a = 224.5 cm = distance between source and point of calculation

R_0 = 26 cm = radius of source

$$\tan \theta = \frac{R_0}{a}$$

Calculation results are given in the following table.

Table 7-13a: Dose rate calculation at the lid for DIDO and MERLIN
fuel assemblies

Point of calculation at the cask	Surface		2 m distance	
E-group (MeV)	1,5	2,0	1,5	2,0
S_V (1/s·cm³)	$2,34 \cdot 10^8$	$9,35 \cdot 10^7$	$2,34 \cdot 10^8$	$9,35 \cdot 10^7$
U (mrem·h^{-1}·sec·cm²)	$2,65 \cdot 10^{-3}$	$3,2 \cdot 10^{-3}$	$2,65 \cdot 10^{-3}$	$3,2 \cdot 10^{-3}$
B (-)	7,36	6,34	7,36	6,34
θ (°C)	46,70	46,70	6,61	6,61
μ_S (cm^{-1})	0,0596	0,0520	0,0596	0,0520
b (-)	12,53	11,13	12,53	11,13
ΔE (θ,b)	$2,51 \cdot 10^{-7}$	$1,09 \cdot 10^{-6}$	$2,27 \cdot 10^{-8}$	$8,89 \cdot 10^{-8}$
D (mrem/h)	9,6	19,9	0,9	1,6
D_{Ges} (mrem/h)	29,5		2,5	

B. RHF fuel assemblies

Calculations must only be carried out for a linear source. Total result D_{GES} is obtained by multiplying by 16. Self shielding is taken into account at the mantle. The calculation model is represented in Fig. 7-4.

$$\tan\theta_1 = \frac{a}{x}; \quad \tan\theta_2 = \frac{a}{x+1}$$

$b_1 \quad = b + \mu_{Fe} \cdot S$

$b \quad$: according to table 7-7

$S \quad$ = thickness of spacer plate = 1.5 cm

- Geometry for dose rate calculation at the surface

$I = H = 202 \quad$ cm = height of source

$a = \quad 16{,}785$ cm = distance between source and cask central axis

$x = \quad 59 \quad$ cm = distance between source and point of calculation

- Geometry for dose rate calculation at 2 m distance

$I = H = 202 \quad$ cm = height of source

$a = \quad 16{,}785$ cm = distance between source and cask central axis

$x = \quad 59 + 200 = 259$ cm = distance between source and point of calculation

The results are displayed below.

Table 7-13b: Dose rate calculation at the lid for 2 RHF fuel assemblies

Calculating point at cask	Surface		2 m distance	
E-group (MeV)	1,5	2,0	1,5	2,0
S_{LS} (1/s·cm)	$3,05 \cdot 10^{10}$	$4,69 \cdot 10^{9}$	$3,05 \cdot 10^{10}$	$4,69 \cdot 10^{9}$
U (mrem·h^{-1}·sec·cm²)	$2,65 \cdot 10^{-3}$	$3,2 \cdot 10^{-3}$	$2,65 \cdot 10^{-3}$	$3,2 \cdot 10^{-3}$
B (-)	7,36	6,34	7,36	6,34
b	12,53	11,13	12,53	11,13
b_1 (-)	13,10	11,63	13,10	11,63
$\triangle F$ (θ, b_1)	$3,53 \cdot 10^{-7}$	$1,57 \cdot 10^{-6}$	$5,68 \cdot 10^{-8}$	$2,48 \cdot 10^{-7}$
D (mrem/h)	0,996	0,708	0,160	0,112
D_{Ges} (mrem/h)	27,3		4,4	

7.5.1.3 Dose rate at the bottom

Calculation is carried out similarly to the way described in chapter 7.3. Dose rate is determined for the central cask axis at the bottom and at a distance of 2 m. The active length is considered as total zone.

A. DIDO and MERLIN fuel assemblies

- Geometry for the calculation of the surface dose rate

H = 266 cm = height of source

a = 21.25 cm = distance between source and point of calculation

R_0 = 26 cm = radius of source

$$\tan \theta = \frac{R_0}{a}$$

- Geometry for the calculation of the dose rate at a distance of 2 m

H = 266 cm = height of source

a = 221.25 cm = distance between source and point of calculation

R_0 = 26 cm = radius of source

$$\tan \theta = \frac{R_0}{a}$$

The results of calculations are given in the following table.

Table 7-14a: Dose rate calculation at the bottom for DIDO and MERLIN fuel assemblies

Calculating point at cask	Surface		2 m distance	
E-group (MeV)	1,5	2,0	1,5	2,0
S_γ (1/s·cm³)	$2,34 \cdot 10^8$	$9,35 \cdot 10^7$	$2,34 \cdot 10^8$	$9,35 \cdot 10^7$
U (mrem·h^{-1}·sec·cm²)	$2,65 \cdot 10^{-3}$	$3,2 \cdot 10^{-3}$	$2,65 \cdot 10^{-3}$	$3,2 \cdot 10^{-3}$
B (-)	6,25	5,41	6,25	5,41
μ_S (cm^{-1})	0,0596	0,0520	0,0596	0,0520
b (-)	11,38	10,12	11,38	10,12
$\triangle E$ (θ,b)	$8,40 \cdot 10^{-7}$	$3,15 \cdot 10^{-6}$	$7,16 \cdot 10^{-8}$	$2,42 \cdot 10^{-7}$
D (mrem/h)	27,3	49,0	2,3	3,8
D_{Ges} (mrem/h)	76,3		6,1	

B. RHF fuel assemblies

Calculation as for the lid.

b_1 = $b + \mu_{Fe} \cdot S$

b = cf. table 7-8

S = 2.275 = equivalent shielding through insert basket bottoms

- Surface

l = H = 202 cm

a = 16.785 cm

- 2m distance

H = 202 cm

a = 16.785 cm

x = 251.75 cm

The results of calculations are shown below.

Table 7-14b: Dose rate calculation at the bottom for 2 RHF fuel
assemblies

Calculating point at cask	Surface		2 m distance	
E-group (MeV)	1,5	2,0	1,5	2,0
S_{LS} (1/s·cm)	$3,05·10^{10}$	$4,69·10^{9}$	$3,05·10^{10}$	$4,69·10^{9}$
U ($mrem·h^{-1}·sec·cm^2$)	$2,65·10^{-2}$	$3,2·10^{-3}$	$2,65·10^{-3}$	$3,2·10^{-3}$
B (-)	6,25	5,41	6,25	5,41
b (-)	11,38	10,12	11,38	10,12
b_1 (-)	12,24	10,87	12,24	10,87
$\triangle E$ (θ,b)	$9,39·10^{-7}$	$3,79·10^{-6}$	$1,42·10^{-7}$	$5,59·10^{-7}$
D (mrem/h)	2,249	1,459	0,340	0,215
D_{Ges} (mrem/h)	59,3		8,9	

7.5.2   Dose rates under accidental conditions

The cement layer dehydrates under accidental conditions. It is conservatively assumed that the layer loses its shielding capacity due to this. The shock absorbers remain on the cask; however, they suffer deformations during an accident, so that they lose part of their shielding capacity. Dose rate calculations were, however, carried out without shock absorbers, so that this has no influence on the results. The usual shielding is remains unchanged. Calculations are carried out assuming a distance of 1 m from the cask.

7.5.2.1   Dose rate at the mantle surface

The maximum dose rate which occurs at the horizontal central plane is determined.

The new value of b is:

(1.5 MeV) b = 11.95 (as compared to 12.15 before)
(2.0 MeV) b = 10.64 (as compared to 10.81 before)

It is evident that the change of shielding capacity as compared to normal transport conditions is small.

All further values are considered to be constant (cf. chapter 7.5.1.1).

A. DIDO and MERLIN fuel assemblies

- Geometry for the calculation of the dose rate at a distance of 1 m
  of the mantle

H = 266 cm = height of source

a = 124.5 cm = distance between source and point of calculation

R_0 = 26 cm = radius of source

$$\tan \theta = \frac{H/2}{a+z}$$

Except for the following values, all others coincide with the values used in 7.5.1.1:

b_1 = 11.95 (1.5 MeV) b_2 = 13.31 (1.5 MeV)
b_1 = 10.64 (2.0 MeV) b_2 = 11.71 (2.0 MeV)

a = 124.5 cm
Z = 22.82 (1.5 MeV) Z = 20.58 (2.0 MeV)

$\Delta F(\theta, b)$ = 5.45 · 10^{-7} (1.5 MeV)

$\Delta F(\theta, b)$ = 2.86 · 10^{-6} (2.0 MeV)

This yields a total dose rate at a distance of 1 m of the mantle of:

D_{GES} = $D_{1.5}$ + $D_{2.0}$

       = 5.2 + 11.4 = 16.6 mrem/h

B. RHF fuel assemblies

- 1m distance

The surface value is calculated by way of simplification.

The new dose rate value at the surface is calculated from:

new $D_{GES} = D_{GES(1.5)} \cdot e^{\Delta b_{1.5}} + D_{GES(2.0)} \cdot e^{\Delta b_{2.0}}$

$\Delta b_{1.5}$ $= 0.2$ (1.5 MeV)

$\Delta b_{2.0}$ $= 0.17$ (2.0 MeV)

D_{GES} $= 22.78 \cdot e^{0.2} + 16.54 \cdot e^{0.17}$

$= 47.4$ mrem/h

The value for a distance of 1 m is lower than the calculated one.

7.5.2.2   Dose rate at the lid

Shielding is not changed under accidental conditions (if the shock absorbers are not taken into account). At the surface and at a distance of 2 m, the same values as in chapter 7.5.2.1 occur. Thus, values for a distance of 1 m are below the defined limit of 1000 mrem/h for all types of loads.

7.5.2.3   Dose rate at the bottom

The same applies for the bottom as for the lid.

7.6   Summary of results

The following tables summarise the calculated dose rates for the TN 7-2 cask, both under normal and accidental conditions.

It can be seen that the maximum dose rates which occur remain below the limits admitted by transport regulations.

Table 7-15a: Dose rates for the TN 7-2 loaded with DIDO and MERLIN fuel assemblies, under normal transport conditions (mrem/h)

Mantle		Lid		Bottom	
Surface	2 m	Surface	2 m	Surface	2 m
38.6	9.4	29.5	2.5	76.3	6.1

Table 7-15b: Dose rates for the TN 7-2 loaded with 2 RHF fuel assemblies, under normal transport conditions (mrem/h)

Mantle		Lid		Bottom	
Surface	2 m	Surface	2 m	Surface	2 m
39.3	6.6	27.3	4.4	59.3	8.9

Table 7-16a: Dose rates at a distance of 1 m of the TN 7-2 loaded with DIDO and MERLIN fuel assemblies, under accidental conditions (mrem/h)

Mantle	Lid	Bottom
16.6	< 29.5	< 76.3

Table 7-16b: Dose rates at a distance of 1 m of the TN 7-2 loaded with 2 RHF fuel assemblies, under accidental conditions (mrem/h)

Mantle	Lid	Bottom
47.4	< 27.3	< 59.3

7.7 Literature

/7-1/ TN 7/MTR Package Design, Safety Report,
    TN report no. 7701

/7-2/ I. O. Blomeke/M. F. Todd:
    U-235 Fission-Product Production as a Function of Thermal
    Neutron Flux, Irradiation Time and Decay Time,
    ORNL 2127, Oak Ridge

/7-3/ Safety Report, Transport of two Irradiated
    RHF Fuel Assemblies in the TN 7 cask,
    TN report no. 8021

/7-4/ T. Rockwell III:
    Reactor Shielding Design Manual, Mc-Graw-Hill Book Company, Inc.
    Princeton-New Jersey (1956)

/7-5/ K. H. Lindackers
    Praktische Durchführung von Abschirmberechnungen,
    Verlag Karl Thiemig KG, München (1962)

/7-6/ R. G. Jaeger:
    Engineering Compendium on Radiation Shielding,
    Vol. I, Springer Verlag, Berlin (1968)

/7-7/ IAEA-Regulations for the Safe Transport of Radioactive Materials, 1973

Stainless steel

Lead

Cement

70

(245)

165

10

25 25 185 10

(245)

17,5

170 (210)

25
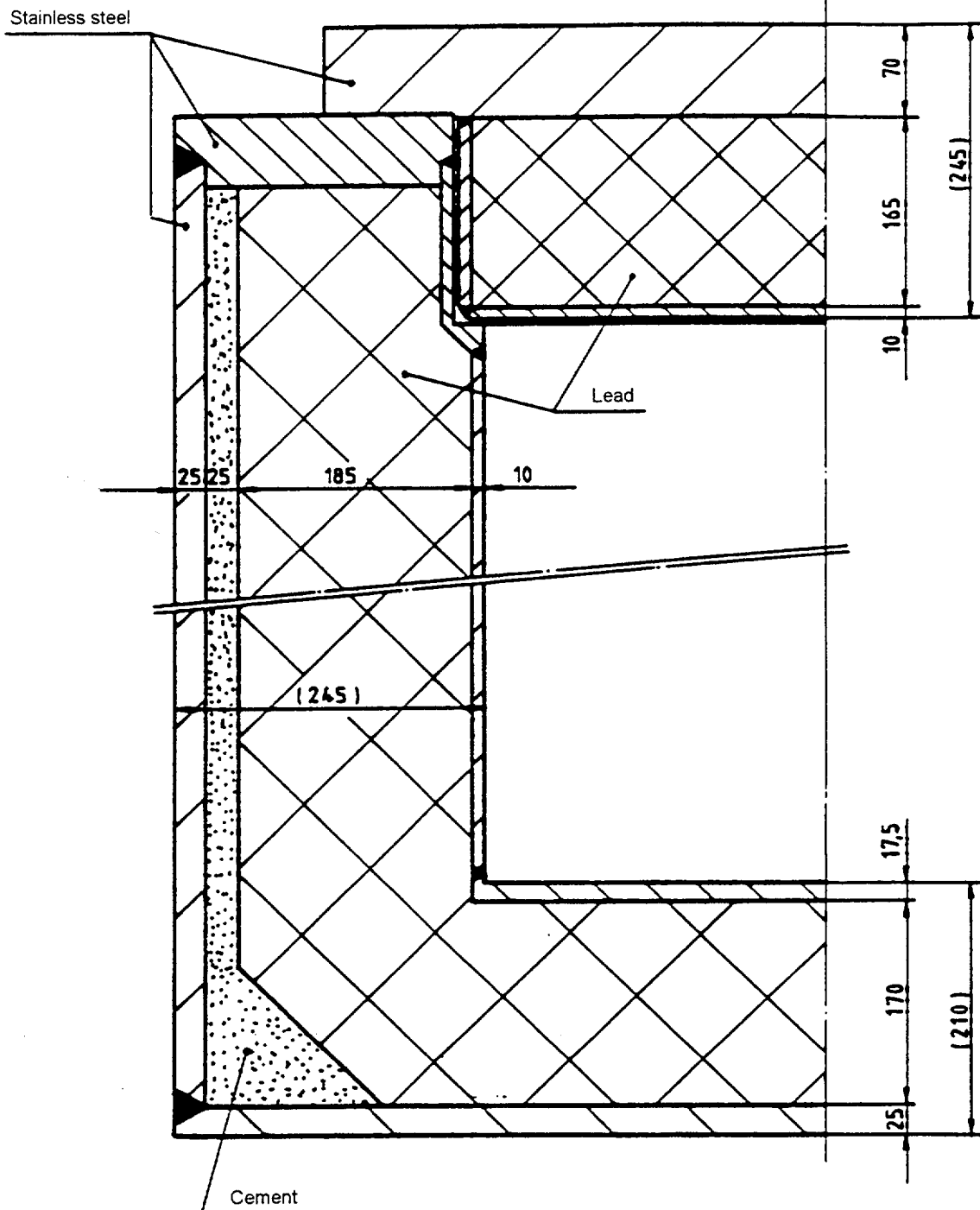
Shielding thicknesses at mantle, lid and bottom of the TN 7-2

Fig. 7-1
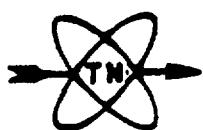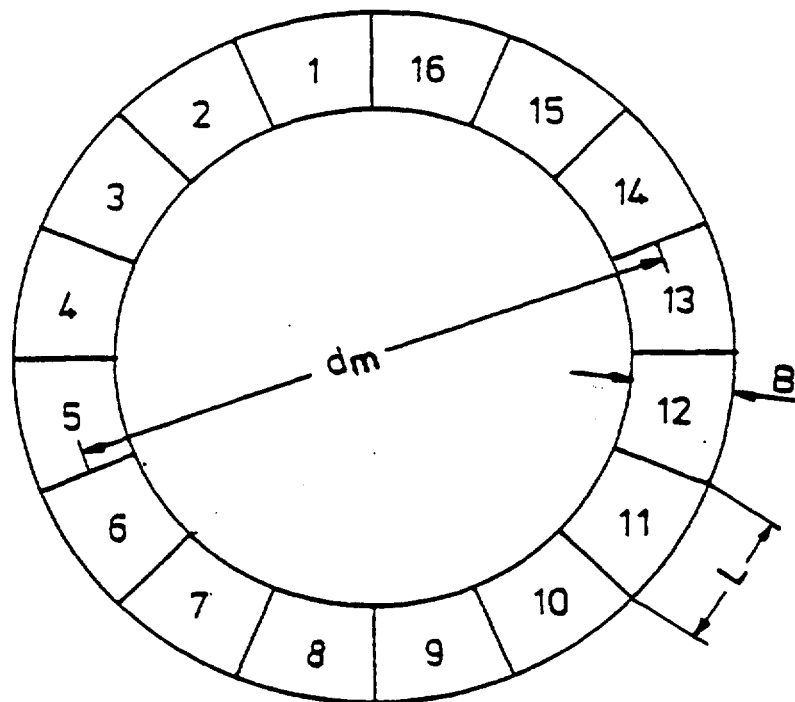
×
Receiving point

Receiving point θ_1

Source

Shielding
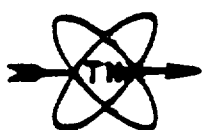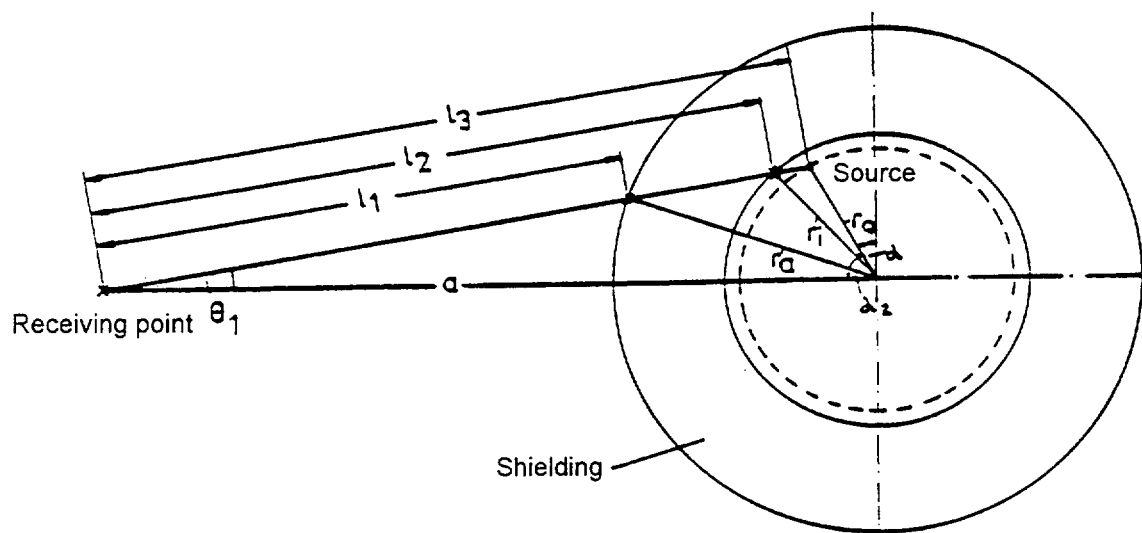
Fig. 7-3
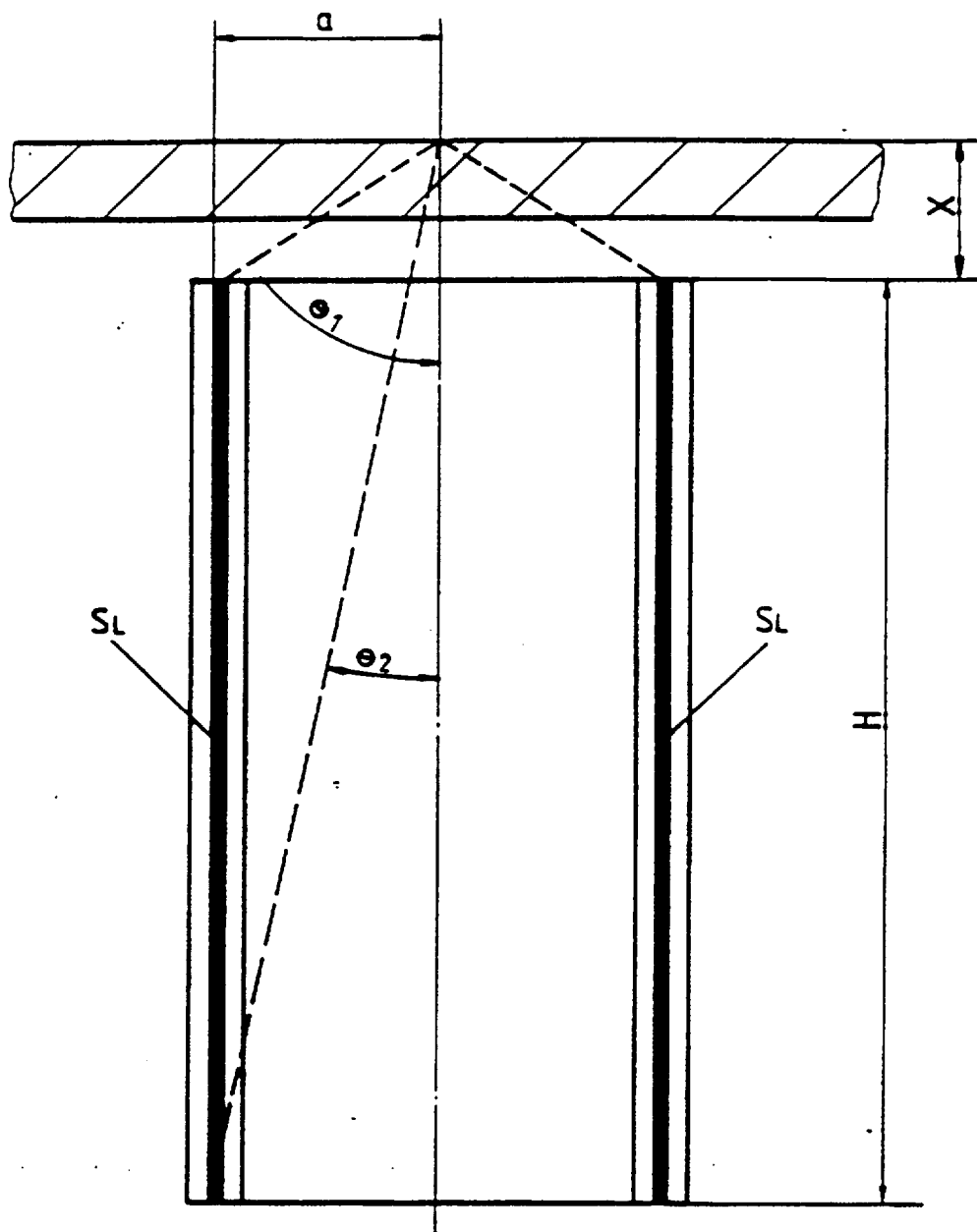
8.   Criticality safety

In the following it will be proven that the TN 7-2 flask,
loaded with the various contents described in Chapter 2,
satisfies the requirements for fissile class II packagings.

8.1   Fundamentals

The nuclear safety of the TN 7-2 flask is based upon the
following factors:

- the fuel elements are as described in Chapter 2.   The
  quantity of fissile material present in the unirradiated
  state will be used for calculation purposes.

- the body of the flask will retain its integrity and
  geometry even under accident conditions.

- the basket is so designed that its geometry will be
  retained under both normal and accident conditions.

8.2   Methods of proof

A. DIDO and MERLIN fuel elements

The baskets used for DIDO and MERLIN fuel elements are
identical to those used in the TN 7.   The usable inner
diameter of the TN 7-2 is also the same as that of the
TN 7 with additional shielding.   The inner length,
however, differs slightly between the two flasks.
These differences are not important for the criticality
safety analysis, as an infinitely long fuel zone is
assumed.

A German package approval issued by the PTB (No.
D/4001/B(U)F (Rev.0)) already exists for transporting
these elements in the TN 7 (described in safety report
/8-1/).

The differences to this package approval with respect
to criticality safety are the following:

1. loading the flask with 2 DIDO and 2 MERLIN baskets
   is proposed, compared with max. 1 MERLIN basket in
   the TN 7.

2. changing the lateral construction of the flask,
   namely:

   - a different material layering sequence

   - varying total layer thicknesses of the individual
     materials (+ 0.5 cm lead, - 1.5 cm steel compared
     with the TN 7).

The first item has no effect on the criticality safety
of the TN 7-2.   This can be proven by the fact that
the criticality safety analysis for the TN 7 flask
assumed a longitudinally infinite fuel zone, both for
DIDO and for MERLIN fuel elements.   This showed that
a load of solely DIDO fuel elements represents the
most reactive state.

In spite of the different layering sequence mentioned
in the second item, there is no change in reactivity
to be expected as the thickness of the layers is
practically identical.

Proof of criticality safety is therefore based on the
following document:

- criticality safety of DIDO and MERLIN fuel elements
  in the TN 7 (H. Krug, University of Munich, 1976),
  annex to the TN 7 safety report (/8-1/).

This report is contained in Appendix 8.1.

B. RHF fuel elements

The basket used in the TN7-2 for 2 RHF fuel elements
is identical to that used in the TN 7.   As far as the
varying packaging geometries of the TN 7 and TN 7-2
are concerned, the remarks made in section 8.2 A apply.

A German package approval for the TN 7 with these
contents (described in /8-2/) has been applied for at
the PTB.
The difference to this package approval lies in reference
to the criticality safety in the present case, in the
change in packaging construction mentioned in section
8.2 A.

Proof of criticality safety is therefore based on the
following document (see Appendix 8.2):

- criticality safety of irradiated RHF fuel elements
  in the TN 7 transport flask (W. Weber, H. Krug, GRS,
  27.4.1982).

8.3   Results

B. RHF fuel elements

The results correspond to those calculated for the
same loading in the TN 7 (see Appendix 8.2).   The
influence of the changed flask geometry is negligibly
small.

The following values were recorded:

- 2 flooded flasks

  For a loading of 2 RHF fuel elements in each flask
  in the given transport state (see Chapter 2)

  $$K_{eff} + \Delta K_{eff} = 0.946 \qquad\qquad \Delta K_{eff} = 2\ \sigma$$

  under full water reflection (30 cm water layer).

- collection of dry flasks

  Any number of dry flasks is sub-critical.

Thus the TN 7-2 flask, loaded with 2 RHF fuel elements,
satisfies the criteria of the nuclear fissile class II.

8.4   References

/8-1/   TN 7 / MTR Package Design, Safety Report,
TN report no. 7701

/8-2/   Safety Report, Transport of 2 irradiated RHF fuel elements
in the TN 7 flask,
TN report no. 8021

CRITICALITY SAFETY

OF DIDO AND MERLIN FUEL ELEMENTS

IN THE TN-7 CASK

(Translation)

Herwin Krug
University of Munich
December 1976

SUMMARY

Criticality safety for the transport of Dido and Merlin type
MTR-elements in the container TN-7 was investigated. An
insert with 15 transport positions out of steel tubes is
foreseen for the round Dido fuel elements and an insert with
16 transport positions consisting of almost square steel
boxes is foreseen for the box-shaped Merlin fuel elements.
Up to four fully laden inserts are to be transported in the
container TN-7, Dido and Merlin inserts being simultaneously
present in the container.

It is shown that the most reactive situation occurs if the
container is completely flooded. The effects of possible
incidents - varying moderation of the fissile material and
decreased water tightness - were investigated for this
situation. It was established that the multiplication factor
of the container is always below 0.9. When the container is
dry, the multiplication factor is under 0.51.

The multiplication factors indicated refer to the flooded or
dry state of containers lying close together in an infinitely
vast arrangement. As a result the transport of Dido and
Merlin fuel elements in the TN-7 with the inserts investiga-
ted has to be classified in the nuclear safety class II.

1. Einführung

The task of investigating the criticality safety of the container TN-7 (Appendix 8.1) for the transport of round MTR fuel elements of the Dido type and of the box-shaped MTR fuel elements of the Merlin type was set. A separate insert is foreseen for each fuel element type. The layout of the inserts is restricted by the useful internal diameter of the TN-7, which is about 54 cm. Since the useful height of the TN-7 is 280 cm, as opposed to 60 cm active length of the fuel elements, up to four inserts can be transported on top of each other in the TN-7. Besides, the transport container should be loaded at one and the same time with inserts for the various fuel element types.

The Dido fuel elements consist of four concentrical rods, made of round, convex fuel plates (Appendix 8.2 and 8.3). The fuel plates themselves are composed of an uranium/aluminium core (layer thickness 0.066 cm) which is encased on both sides by an aluminium layer (0.0425 cm each). In all, a Dido fuel element contains 185 g U-235, with a degree of enrichment between 80 and 93 % and uranium core content of about 17-18 %. However, during transport the rods of the Dido fuel elements are not concentric; the rods in each fuel element are secured together at one side (Appendix 8.4).

The insert for the Dido fuel element contains 15 transport positions. The transport positions are in the form of steel rods with an internal diameter of 10.4 cm and a wall thickness of 0.5 cm. These rods are fixed in two concentric circles on an annular spacing structure (figure 1). However, it can be seen from the critical analysis of the Dido insert which follows, that these dimensions are of minor importance only.
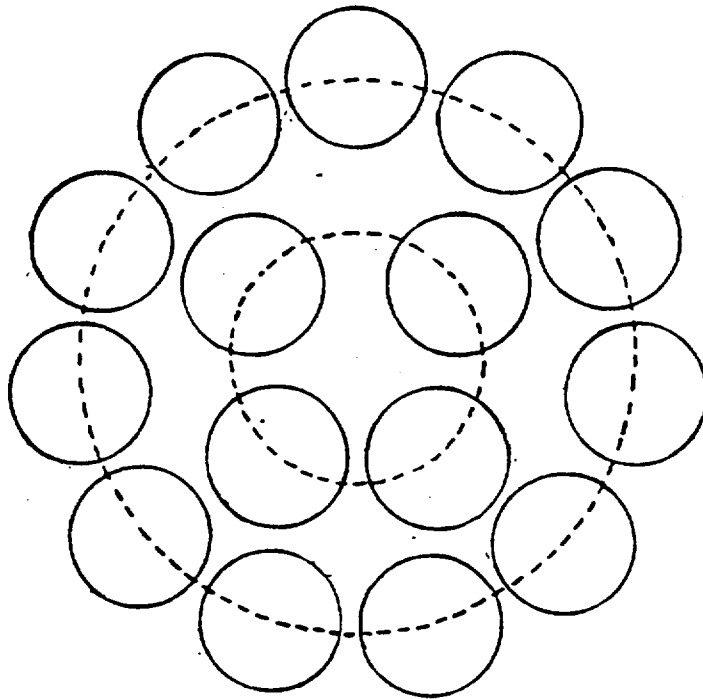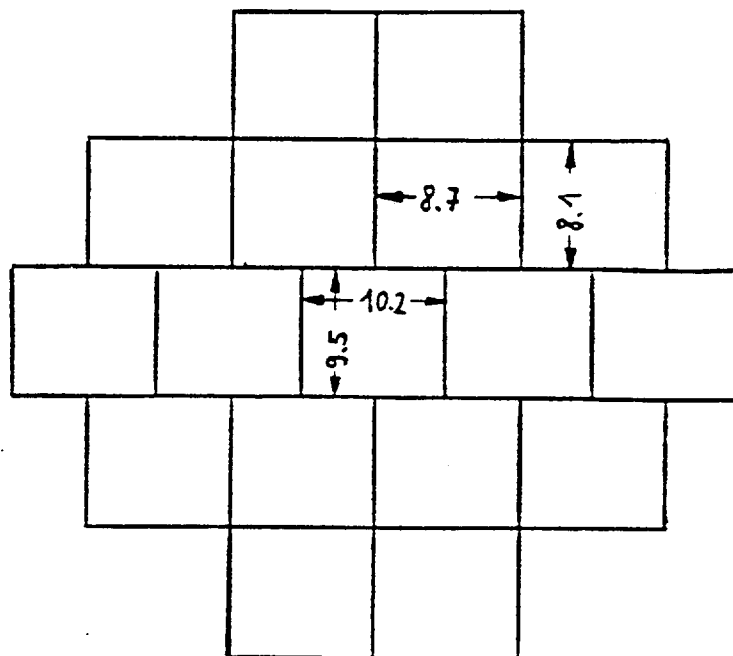
Figure 1 : DIDO insert

Figure 1 : MERLIN insert

The Merlin fuel elements are an example of classical box-
shaped MTR fuel elements with more or less square cross-
section (Appendix 8.5, 8.6 and 8.7). The Merlin fuel elements
contain 270 g U-235, likewise with a degree of enrichment
between 80 and 93 %. The Merlin fuel plates themselves are
composed of an uranium/aluminium core (layer thickness 0.051
cm), encased by an aluminium layer (0.038 cm each) on both
sides. The uranium content in the core amounts to about 21 to
27 %.

The insert for the Merlin fuel elements contains 16 transport
positions. The transport positions are in the form of almost
square steel boxes lying close together (inner dimensions
8.7 cm x 8.1 cm) with a wall thickness of 0.7 cm. The rela-
tionship of the steel boxes to an insert is clearly visible
from figure 2. Steel poisoning is foreseen neither for the
Dido nor for the Merlin fuel element inserts.

In order to judge the criticality safety in the cases mentioned
above, the container flooded state is of decisive importance,
as the highest reactivity can be reached here. Consequently
the following criticality analysis is primarily concerned with
the flooded state. In addition, an arrangement of dry con-
tainers is also examined, as differing conditions can occur
with respect to neutron interaction.

2. Calculating method - General assumptions

The method of calculation applied, which is particularly adapted to the flooded state of the container, can be divided into three main steps :

1. determination of the cross-sections for the active zones and structure materials

2. determination of homogenized cross-sections for the various basket lattice cells

3. determination of the loaded container with the various basket lattice cells.

This method of calculation, which suggests itself thanks to the arrangement of the transport positions in the inserts, has proved to be of particular value for the calculation of transport containers (Ref. 1 and 2). The group constants for fuel element areas and structural materials were calculated with the GAMTEC programme (Ref. 5). For the determination of fast group constants the B-1 approximation was used, for the determination of the thermal group constants of the fuel zones the Wigner-Wilkins approximation using water moderation and of structural materials a Maxwell distribution. These group constants all related to room temperature and a geometric buckling of 1.10^{-4}.

For the determination of nuclide densities the following values were uniformly applied: water, 1.0 g . cm^{-3}; lead, 10.77 g . cm^{-3} and for steel 7.566 g . cm^{-3} (composition according to DIN 1.4301 ≙ X5CrNi 189 ≙ SS - 304). The densities for lead and steel in the calculation are only 95 and 97 % respectively of the actual densities, in order to take density changes such as may occur through fabrication variations and thermal expansion conservatively into consideration.

The group constants, which are homogenized for the transport positions, were produced by the multi-group diffusion programme CITATION (Ref. 6).   The container calculations were also carried out with the CITATION programme. A local flux convergence of 10^{-3} was asserted for all CITATION calculations. All calculations in the flooded state were carried out with four neutron groups. The four group standard set-up for light water reactors (10 MeV - 8.21 KeV - 5.53 KeV - 0.625 eV - 0.0 eV) was used as group classification.

For the criticality analysis of dry containers the Hansen-Roach cross-section for 16 neutron groups, especially devised for hard neutron spectra, was used (Ref. 3). Determination of the reactivity was carried out by the Monte-Carlo programme KENO (Ref. 7).

3. Flooded container with DIDO fuel elements

3.1 Group constants for DIDO fuel elements

As the degree of enrichment given for DIDO fuel elements
was only between 80 and 93 %, it was conservatively assumed
that the entire uranium was present in the form of U-235,
in order to cover the whole range of enrichment. In parti-
cular a uranium quantity of 200 g U-235 per fuel element
was taken as a basis. Assuming a full material density for
U-235 (g = 18.662 g · cm^{-3}) and for aluminium (g = 2.698 g
· cm^{-3}) the uranium content in the core was calculated at
17.738 %. This results in the following nuclide densities:

1) Core   U-235 = $0.14459 \cdot 10^{-2}$ $b^{-1} \cdot cm^{-1}$
                 Al   = $0.58401 \cdot 10^{-1}$ $b^{-1} \cdot cm^{-1}$

2) Al-cladding   Al   = $0.60222 \cdot 10^{-1}$ $b^{-1} \cdot cm^{-1}$

Fluctuations in the uranium content in the core are only
noticeable with a constant uranium quantity (200 g) in the
nuclide density for aluminium. Minor fluctuations in the
nuclide density of aluminium are caused by insignificant
reactivity changes in the fuel elements, as was shown in an
experiment on MERLIN fuel plates of similar structure,
described in section 4.1.

For further calculations, the fuel plates were homogenized
with the surrounding water, an approach which led to con-
servative results with highly enriched uranium. For this
homogenization only the active part of the fuel plates was
used. Since no clear-cut volume or fixed water or moderator
percentages can be attributed to the DIDO fuel elements in
a transport position because of the layout of the fuel rods

(Appendix 8.4), a series of calculations was carried out, in which areas of transport positions of varying sizes were homogenized. In Table 1 those measurements, resulting from these calculations, are listed which enable an easy assessment of the reactivity of the fuel elements with varying homogenization volumes.

Table 1

% Vol	R /cm/	K_∞	B_m^2	τ	L^2	p	$(\eta f)_1$	$(\eta f)_2$
100	5.2	1.5623	.0156	31.799	2.9602	.95581	1.2232	1.578
90	4.9332	1.6008	.0164	32.553	2.8431	.95126	1.2545	1.618
80	4.6510	1.6408	.0170	33.541	2.7272	.94534	1.2874	1.661
70	4.3506	1.6820	.0175	34.899	2.6167	.93731	1.3221	1.706
65	4.1924	1.7030	.01769	35.786	2.5659	.93212	1.3401	1.729
60	4.0279	1.7240	.01775	36.875	2.5207	.92580	1.3586	1.753
55	3.8564	1.7450	.01768	38.246	2.4828	.91796	1.3775	1.777
50	3.6770	1.7656	.0174	40.021	2.4591	.90795	1.3970	1.803
40	3.2888	1.8033	.0162	45.802	2.4874	.87646	1.4373	1.854

In the first column the percentual volume of the transport position is given, on which the homogenization was based. 100 % implies homogenization of the whole transport position or of the whole available internal surface of a rod in the insert. In column 2 the corresponding equivalent radius of the fuel element volume with an active height of 60 cm is given.

3.2 Group constants for DIDO basket lattice cells

From Table 1 it cannot be seen which fuel element data give
the most reactive group constants for the basket lattice
cell. This is due to the fact that neither the reactivity
effect on the water particles remaining in the basket
lattice cell nor the reactivity effect of neutron absorption
in the steel tube of the transport position can be estimated
because of the internal neutron flux. Consequently group
constants for the corresponding basket lattice cells were
calculated for all fuel element data. In the calculating
model the basket lattice cell was described as a cylindrical
fuel element zone with radius R_{BE}, a water ring zone of
ΔR_{H_2O} and steel tube transport position (0.5 cm). As
limiting condition full reflection ($\nabla \emptyset = 0$) was assumed on
the outer surface of the tube. This assumption leads to
conservative results as will be shown later in this chapter.

Table 2

% Vol	R_{BE}	$\Delta\,R_{H2O}$	K	B^2_M	τ	L^2
100	5.2	0.0	1.1209	.00321	35.096	2.544
90	4.9332	0.2668	1.1131	.00301	35.093	2.528
80	4.6510	0.5490	1.0946	.00251	35.106	2.531
70	4.3506	0.8494	1.0645	.00171	35.146	2.558
65	4.1924	1.0076	1.0449	.00119	35.180	2.584
60	4.0279	1.1721	1.0217	.00057	35.226	2.619
55	3.8564	1.3436	.9949	÷00013	35.288	2.665
50	3.6770	1.5230	.9639	÷00095	35.371	2.726
40	3.2888	1.9112	.8874	÷00292	35.629	2.907

Table 2 shows that the most reactive group constants for
the basket lattice cells occur throughout the entire trans-
port position during homogenization.

The most reactive group constants for the active zone with
regard to material buckling occur in an active zone com-
posed of 60 % volume of the transport position (table 1).
It was therefore investigated whether in this case a more
reactive basket cell is formed with an other than cylindri-
cal fuel arrangement in the transport position. The
calculating model for this is different from the previous
one, in so far as the fuel is assumed to be in a circle in
the basket lattice cell. The central water volume was
increased from 0 to 40 % volume of the transport position,
i.e. until the active zone inside finally touches the tube
lining of the transport position. The results are given in
table 3.

Table 3

% Vol	R_{H2O}	ΔR_{BE}	ΔR_{H2O}	K_∞
0	0.0	4.0279	1.1721	1.0217
5	1.1628	3.0295	1.0077	1.0456
10	1.6444	2.7062	0.8494	1.0582
20	2.3255	2.3255	0.5490	1.0589
30	2.8482	2.0849	0.2669	1.0335
40	3.2888	1.9112	0.0	0.9861

In the first column the central water volume is given as a
percentage volume of the transport position. In the follow-
ing columns the radius of the central water volume, as well
as the thickness of the corresponding circular active and
water zones respectively is given in cm. It can be seen
from table 3 that the multiplication factor for a central
water volume of about 20 % reaches a maximum. The reacti-
vity of the basket lattice cell, even in this case, is well
below the value obtained by homogenizing the fuel element
over the whole transport position (table 2). For future
experiments, it will always be assumed that the fuel element
is homogenized for the whole transport position.

In the calculations made to date, an outer water layer in the
basket lattice cells was not taken into account. Consequent-
ly a whole series of calculations was made, for which the
basket lattice cell was extended by an outer circular layer
of water. For this, the water layer varied between 0 and
2.0 cm.

The results are given in table 4.

Table 4

R_{H2O}	R_{Cell}	K_∞	B^2_M	τ	L^2
0.0	5.7	1.1209	.00321	35.096	2.544
0.1	5.8	1.0969	.00260	34.655	2.557
0.2	5.9	1.0740	.00201	34.251	2.576
0.285	5.985	1.0554	.00152	33.934	2.596
0.5	6.2	1.0111	.00031	33.223	2.664
1.0	6.7	0.9191	-.00232	31.962	2.904
1.271	6.971	0.8739	-.00365	31.447	3.069
2.0	7.7	0.7652	-.00690	30.445	3.582

In the first column the thickness of the outer water layer
is given, and in the second column the resulting cell radius.
It can be seen from table 4 that the reactivity of the
basket lattice cell decreases sharply as the outer water
layer increases. Mention should be made of two further
examples which are apparent from table 4. An outer water
layer of 0.285 cm corresponding to the case where all trans-
port positions lie close together in a hexagonal lattice,
i.e. there is the smallest possible lattice pitch. An outer
water layer of 1.271 cm corresponds to a basket lattice cell
resulting from a uniform distribution of the transport posi-
tions in the transport container. This case is the closest
to the conditions which actually prevail.

3.3 DIDO inserts in the TN-7

The determination of the TN-7 reactivity was not based on a
definite number of inserts, an infinite extension of the con-
tainer with insert and fuel elements in an axial direction
was conservatively assumed. The radial structure of the
TN-7 is illustrated in Appendix 6.1.

In the calculation the radial structure was described by
layers of steel (1 cm), lead (5 cm), steel (2 cm), lead
(13 cm), steel (2 cm), lying close together, with a free
internal radius of 27 cm.

The insert with the fuel elements was represented by a co-
axial cylindrical zone, whose cross-section is equal to
the surface area of all the basket lattice cells. The
multiplication factor for the basket lattice cells of vary-
ing sizes, which differed only in their outer water layer
(table 4), was calculated, assuming full reflection
($\nabla \emptyset = 0$) as limiting condition on the outer wall of the
container. This limiting condition gives conservative
results, as will be shown in this chapter. The results of
this calculation are given in table 5. In the first column
is the cell radius, R_{cell} of the basket lattice cell which
forms the insert; in the second column is the equivalent
insert radius R_{insert} and in the 3rd column, in cm, the
water layer thickness ΔR_{H2O} between the insert and the
inner wall of the container.

Table 5

R_{Cell}	R_{Basket}	ΔR_{H2O}	K_∞
5.7	22.076	4.924	0.8980
5.8	22.463	4.538	0.8884
5.9	22.851	4.149	0.8791
5.985	23.180	3.820	0.8715
6.2	24.012	2.988	0.8532
6.7	25.949	1.051	0.8136
6.971	27.0	0.0	0.7896

It can be seen from table 5 that the container reactivity
decreases sharply as the size of the basket lattice cells
increase, i.e. with increasing outer water layer around the
transport position. K_∞ values for basket lattice cells
with a radius of less than 5.985 cm are of purely mathemati-
cal significance since - as already mentioned - the smallest
possible distance between the steel tubes forming the trans-
port positions would be surpassed.

The multiplication factors in table 5 are based on full
neutron reflection on the outer container wall. Consequent-
ly the reactivity influence of an outer water layer was
investigated. For this purpose the container calculating
model was extended outside by an adjacent circular layer of
water. This water layer ΔR_{H_2O} was varied between 0 and
30 cm. Full reflection was again assumed as limiting condi-
tion. The basket lattice cell with radius of 5.985 cm or
insert with equivalent radius of 23.18 cm respectively
table 5) was conservatively taken for these calculations.
The results can be seen in table 6.

Table 6

ΔR_{H_2O}	0.0	1.0	2.0	4.0	8.0	15.0	30.0
K_∞	0.8715	0.8603	0.8581	0.8567	0.8563	0.8563	0.85

From this table it can be seen that the reactivity drops as
the outer water layer thickness increases, i.e. that the
assumption of full reflection on the outer container wall
leads to conservative results. From the very slight de-
crease in K_∞ it can be concluded that TN-7 containers are
almost completely neutralized against each other as far as
neutrons are concerned, thanks to the container structure.

4. Flooded container with MERLIN fuel elements

4.1 Group constants for MERLIN fuel elements

Analogous with DIDO fuel elements, it was likewise assumed for MERLIN fuel elements that the entire uranium was present in the form of U-235. In particular, a basic uranium quantity of 290 g U-235 per fuel element was taken. Because of the high fluctuation of the aluminium content in the core, the reactivity effect of the aluminium in the core was investigated for uranium core contents of 21, 22, 25 and 30 %. With a constant uranium content of 290 g U-235 the corresponding aluminium values can be calculated. When one compares these values with the total active volume of the fuel plates, the following nuclide densities result in the core :

$$
\begin{array}{lll}
\text{U-235} & = 0.17524 \cdot 10^{-2} \ b^{-1} \cdot cm^{-1} \\
\text{Al (U = 21 \%)} & = 0.58066 \cdot 10^{-1} & \text{"} \\
\text{Al (U = 22 \%)} & = 0.54112 \cdot 10^{-1} & \text{"} \\
\text{Al (U = 25 \%)} & = 0.45787 \cdot 10^{-1} & \text{"} \\
\text{Al (U = 30 \%)} & = 0.35612 \cdot 10^{-1} & \text{"}
\end{array}
$$

The same aluminium thickness as for DIDO fuel plates was assumed for the cladding.

For the determination, the fuel plates were homogenized similarly to the DIDO fuel plates. Contrary to the DIDO fuel element, a definite homogenization volume can be attributed to the MERLIN fuel element due to the constant lattice pitch of 0.342 cm. However, with regard to incidents such as compaction of the fuel plates or increase in the lattice pitch through dislocation, the reactivity effect caused by alteration of the lattice pitch or the

homogenized volume respectively was examined closely.
In particular, a lattic pitch of 0.171 cm corresponding
to an effective fuel element expanse of 6.3 x 3.76 cm^2,
if fuel plate compaction occurred, was considered.
Should expansion occur, fuel element expanses of
7.56 x 7.56 cm^2, 7.96 x 7.96 cm^2 and 8.7 x 8.1 cm^2 were
investigated. With regard to the homogenization of the
fuel plates, this corresponds to effective lattice
pitches of 0.413 cm, 0.458 cm and 0.508 cm. Characteristic
reactivity values for these calculations are given in
table 7. It can be seen from this table that a uranium
content of ca. 21 % in the core gives the most reactive
values with reference to material buckling, whereas if the
uranium content increases the rise in the multiplication
factor is negligible. As a result, only group constants
with a uranium content of 21 % in the core are used for
the basket lattice calculations.

Table 7

| BE	%U-235	K_∞	B^2_m	τ	L^2	P	$(\eta f)_1$	$(\eta f)_2$
0.171a	21%	1.7743	0.0067	111.68	4.0919	0.57188	1.5264	1.9599
23.701b	22%	1.7761	0.0066	113.63	4.1116	0.57200	1.5282	1.9615
33.63%c	25%	1.7798	0.0064	118.00	4.1535	0.57225	1.5320	1.9650
6.3x3.76d	30%	1.7843	0.0061	123.84	4.2049	0.57255	1.5366	1.9692
0.342a	21	1.8091	0.0171	43.626	2.3038	0.87726	1.4426	1.8604
47.401b	22	1.8105	0.0170	44.000	2.3069	0.87734	1.4440	1.8618
67.26%c	25	1.8135	0.0168	44.812	2.3138	0.87750	1.4468	1.8647
6.3x7.52d	30	1.8172	0.0165	45.848	2.3229	0.87770	1.4503	1.8683
0.413a	21	1.7791	0.0182	39.289	2.3038	0.90361	1.4099	1.8185
57.229b	22	1.7804	0.0181	39.568	2.3067	0.90368	1.4112	1.8198
81.21%c	25	1.7833	0.0179	40.168	2.3125	0.90381	1.4139	1.8220
7.56x7.56d	30	1.7868	0.0176	40.929	2.3200	0.90397	1.4171	1.8260
0.458a	21	1.7584	0.0184	37.515	2.3347	0.91473	1.3900	1.7923
63.423b	22	1.7597	0.0183	37.755	2.3380	0.91478	1.3912	1.7941
90.00%c	25	1.7625	0.0182	38.270	2.3433	0.91490	1.3938	1.7968
7.96x7.96d	30	1.7659	0.0180	38.920	2.3500	0.91505	1.3969	1.8000
0.508a	21	1.7343	0.0185	36.003	2.3852	0.92435	1.3679	1.7643
70.47b	22	1.7356	0.0184	36.210	2.3877	0.92440	1.3691	1.7658
100%c	25	1.7383	0.0183	36.653	2.3929	0.92451	1.3715	1.7683
8.7x8.1d	30	1.7415	0.0181	37.211	2.3990	0.92464	1.3746	1.771

a : lattice pitch
b : fuel-element surface
c : % volume fuel element to transport position
d : fuel element dimensions in cm

4.2 Group constants for MERLIN basket lattice cells

In accordance with the construction of the insert (fig. 2)
the almost square transport position box was considered as
basket lattice cell (fig. 3) and the limiting condition of
full reflection ($\nabla \emptyset = 0$) was assumed. Furthermore, a
centrical location for the fuel element was supposed. Due
to the resulting symmetry, the calculating model could be
restricted to a quarter representation of the basket
lattice cell. The reciprocal transfer of the transport
positions was not taken into consideration in this calcu-
lating model. However, it is shown in Ref. 1 that
reciprocal transfer has practically no effect on the group
constants.

Figure 3
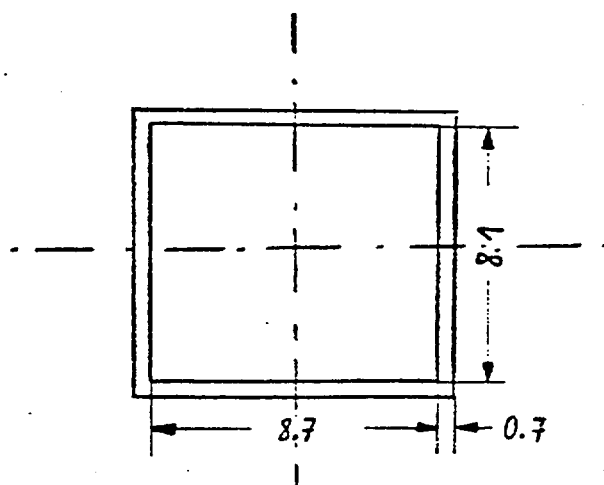
The assumption of full reflection on the outside should be
judged conservatively as each transport position has water
on at least one side. This was established from the
calculations previously made for DIDO fuel elements. For
the active zones which deviate sharply from a square cross-
section (6.3 x 3.76 cm^2 and 6.3 x 7.52 cm^2) both possible
positions in a centrical arrangement in the transport
position were examined.

The calculating models for the fuel elements of various
dimensions and the results are assembled in figure 4. In
cases 1 and 2, the broken lines indicate the possible alter-
native positions; the corresponding results are given in
brackets. It can be seen from figure 4 that the most
reactive group constants occur throughout the whole trans-
port position when the fuel element is homogenized, whereas
the reactivity of the basket lattice cell diminishes as the
fuel element cross-section or homogenized volume respective-
ly decreases. This implies that compacted fuel elements
lead to lower multiplication factors.

As already mentioned, a centrical location for the fuel
element was always supposed in the transport position.
However, an excentrical location of the fuel element does not
generally increase the reactivity (Ref. 1). This is due to
the fact that the negative reactivity effect from the
increase in the water column between the fuel element and
the basket wall outweighs the positive reactivity effect from
the reduction in the water column on the opposite side of the
fuel element. This effect can be seen equally well from
fig. 4, cases 1 and 2. The fuel elements drawn in broken
lines lie with one side nearer to the basket wall and there-
fore result in less reactive basket lattice cells.

4.3 MERLIN inserts in the TN-7

Analogous to the DIDO inserts, an infinite extent of MERLIN
inserts with fuel elements and of the container was assumed
here, in axial direction. The radial container structure
was retained (chapter 3.3). Full reflection ($\nabla \emptyset = 0$) was
assumed on the outer wall of the container. The conservati-
vity of this assumption was already pointed out in chapter
3.4.

Figure 4

1. Fuel element 6.3 x 3.76 cm^2
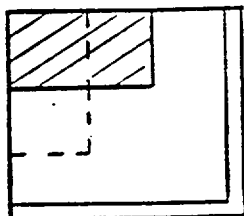
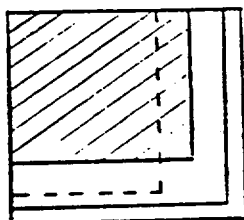K_∞ = 0.7836 (0.7710)

M^2 = 48.439 (48.580)

B_m^2 = -.0045 (-.0047)

2. Fuel element 6.3 x 7.52 cm^2

K_∞ = 1.0990 (1.0866)

M^2 = 45.050 (45.039)

B_m^2 = 0.0022 (0.0019)

3. Fuel element 7.56 x 7.56 cm^2
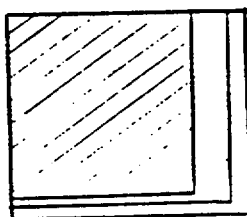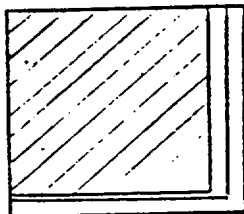

K_∞ = 1.1626

M^2 = 44.675

B_m^2 = 0.0036

4. Fuel element 7.96 x 7.96 cm^2

K_∞ = 1.1890

M^2 = 44.669

B_m^2 = 0.0042

5. Fuel element 8.7 x 8.1 cm^2
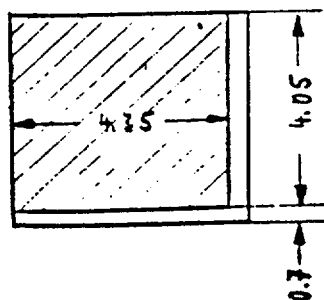
K_∞ = 1.2095

M^2 = 44.617

B_m^2 = 0.0047

The insert was represented as a co-axial circular zone in the container, corresponding to its construction (fig. 2) for the calculation. The inner radius of this zone results from the radius of the cylinder which has an equal surface area to the central water hole (R_i = 5.56 cm). The outer radius is determined by analogy with the surface area of the 16 basket cells (R_a = 22.79). This cylindrisation leads to conservative results, since the surface to volume ratio and subsequently the neutron leakage in the surrounding water is reduced (Ref. 1). The multiplication factor of the container was calculated for each basket lattice cell illustrated in fig. 4. The results are given in table 8.

Table 8

BE	6.3 x 3.76	6.3 x 7.52	7.56 x 7.56	7.96 x 7.96	8.7 x 8.
K_B	0.5765 (0.5662)	0.8241 (0.8138)	0.8732	0.8930	0.9078

The multiplication factors in brackets correspond once again to the alternative fuel element locations in the transport positions. As the MERLIN fuel element, contrary to the DIDO fuel element, can be attributed with a fixed cross-section of 6.3 x 7.52, a multiplication factor of 0,8241 should be applied in this instance in order to judge the criticality safety. Compaction of the fuel element causes a sharp reduction, and expansion of the fuel element an increase, in the container multiplication. At any rate, the case with a fuel element dimension of 8.7 x 8.1 cm^2 is more of mathematical significance, as in practice it can never arise. Considering the accumulation of conservativities, the actual multiplication factor in this case will also be below 0.9.

Furthermore, the reactivity effect of manufacturing
tolerances for the MERLIN insert in the container was
investigated. The surface cross-section of the central
water hole (F = 97.09 cm^2) was taken as parameter. An
average reactivity coefficient $K_B^{-1} \cdot \triangle K_B / \triangle F$ = $-3.8 \cdot 10^{-4}$
resulted uniformly throughout the container with the
various basket lattice cells (fig. 4). Diminishing of
the central water hole increases, and increasing of the
central water hole therefore reduces, the container multi-
plication. Because this reactivity coefficient is so low,
this effect is not of importance for criticality safety
with the normal fabrication variations.

5.   DIDO and MERLIN inserts in the TN-7

Loading of the TN-7 simultaneously with DIDO and MERLIN inserts
presents no particular criticality safety problem. The multi-
plication factor lies between those for the container when fully
laden with DIDO or MERLIN inserts respectively. This is due to
the fact that neutrons from the more reactive zone diffuse to
the less reactive zone. To illustrate this point another sample
calculation was performed. The calculating model for this is
generally of cylindrical geometry and is illustrated in fig. 5.
For the calculating model an infinite range of alternate DIDO
and MERLIN inserts in axial direction was taken.

Figure 5
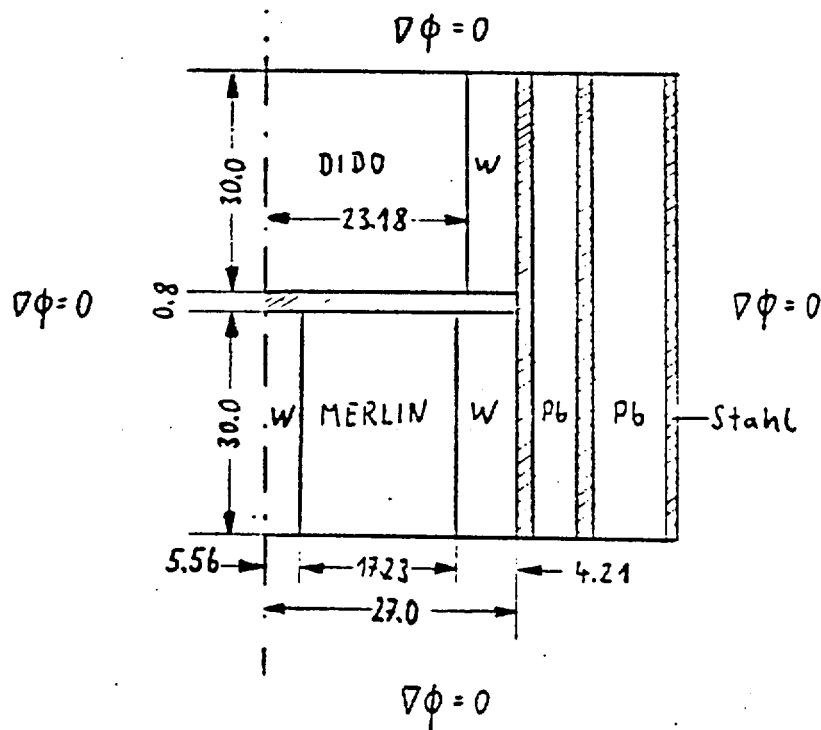
Between the inserts, as provided for in practice, a steel plate
(0.8 cm thick) was taken into account. The actual container
structure was retained. The DIDO insert corresponds to the
case of rods lying close together after homogenization of the
fuel elements throughout the transport position. The MERLIN
insert corresponds to the basket lattice, case 2 in figure 4.
A multiplication factor of 0.8402, i.e. between the values
for the DIDO insert (0.8715) and for the MERLIN insert (0.8241)
was determined for this arrangement.

6. Temperature influence

The experiments were carried out up till now at room temperature. In principle, higher temperatures are only noticeable with the available fissile material systems through a reduction in density, due to the thermal expansion on the reactivity. In the flooded state, the water density is the decisive element for reactivity. Consequently, the case of reduced water density was investigated for both fuel element and basket types. In particular, water densities of 0.9 and 0.8 g · cm^{-3} in the respective active zones were taken. The geometrical dimensions were retained unchanged, so that the uranium and aluminium densities remained the same.

For the DIDO fuel elements group constants corresponding to the assumptions presented in chapter 3.1 for both reduced water densities were calculated again. The most important characteristic criticality measurements, deduced from these calculations, are given in table 9. From table 9 it can be seen that the K_∞ increases with decreasing water density, but that the material buckling also decreases. This is due to the fact that the increase in the migration area M^2 is more noticeable for material buckling.

Which effect in the end has the greatest influence on the container multiplication factor can only be established by further calculations. As a result, more group constants for the DIDO basket lattice cells similar to those shown in chapter 3.2, table 2 were calculated. For this, the water density in the active zone was reduced, whilst the water density in the ring between the active zone and the steel rod of the transport position was conservatively retained. The characteristic criticality measurements resulting from these calculations are given in table 10. From table 10 it can be seen that the

Table 9

% Vol	$\rho-H_2O$	K_∞	B_m^2	τ	L^2	M^2
	1.0	1.5623	.0156	31.799	2.960	34.759
100	0.9	1.5946	.0136	38.644	3.411	42.055
	0.8	1.6279	.0116	47.975	3.995	51.970
	1.0	1.6008	.0164	32.553	2.843	35.396
90	0.9	1.6303	.0142	39.491	3.275	42.766
	0.8	1.6605	.0121	48.920	3.831	52.751
	1.0	1.6408	.0170	33.541	2.727	36.268
80	0.9	1.6671	.0147	40.601	3.137	43.738
	0.8	1.6938	.0124	50.166	3.670	53.836
	1.0	1.6820	.0175	34.899	2.617	37.516
70	0.9	1.7047	.0151	42.125	3.009	45.134
	0.8	1.7275	.0127	51.870	3.517	55.387
	1.0	1.7030	.0177	35.786	2.566	38.352
65	0.9	1.7237	.0152	43.122	2.950	46.072
	0.8	1.7443	.0127	52.986	3.447	56.433
	1.0	1.7240	.0177	36.875	2.521	39.396
60	0.9	1.7426	.0152	44.344	2.896	47.240
	0.8	1.7608	.0127	54.357	3.384	57.741
	1.0	1.7450	.0177	38.246	2.483	40.729
55	0.9	1.7612	.0151	45.881	2.854	48.735
	0.8	1.7769	.0127	56.086	3.335	59.421
	1.0	1.7656	.0174	40.021	2.459	42.480
50	0.9	1.7792	.0149	47.870	2.825	50.695
	0.8	1.7921	.0125	58.318	3.300	61.618
	1.0	1.8033	.0162	45.802	2.487	48.289
40	0.9	1.8109	.0138	54.348	2.857	57.205
	0.8	1.8174	.0116	65.602	3.332	68.934

Table 10

% Vol	ρ-H_2O	K_∞	B_m^2	τ	L^2	M^2
100	1.0	1.1209	.00321	35.096	2.544	37.640
	0.9	1.1259	.00281	41.967	2.844	44.811
	0.8	1.1290	.00237	51.090	3.222	54.312
90	1.0	1.1131	.00301	35.093	2.528	37.621
	0.9	1.1149	.00261	41.172	2.809	43.981
	0.8	1.1150	.00221	48.907	3.161	52.068
80	1.0	1.0946	.00251	35.106	2.531	37.637
	0.9	1.0931	.00216	40.287	2.790	43.077
	0.8	1.0895	.00179	46.883	3.116	49.999
70	1.0	1.0645	.00171	35.146	2.558	37.704
	0.9	1.0598	.00141	39.549	2.796	42.345
	0.8	1.0529	.00110	45.007	3.094	48.101
65	1.0	1.0449	.00119	35.180	2.584	37.764
	0.9	1.0384	.00091	39.203	2.811	42.014
	0.8	1.0303	.00064	44.125	3.094	47.219
60	1.0	1.0217	.00057	35.226	2.619	37.845
	0.9	1.0140	.00034	38.873	2.835	41.708
	0.8	1.0046	.00010	43.278	3.104	46.382
55	1.0	.9949	-.00013	35.288	2.665	37.953
	0.9	.9860	-.00034	38.563	2.871	41.434
	0.8	.9756	-.00053	42.469	3.127	45.596
50	1.0	.9639	-.00095	35.371	2.726	38.097
	0.9	.9542	-.00111	38.277	2.921	41.198
	0.8	.9431	-.00127	41.697	3.163	44.860
40	1.0	.8874	-.00292	35.629	2.907	38.536
	0.9	.8768	-.00301	37.800	3.083	40.883
	0.8	.8652	-.00309	40.287	3.301	43.588

migration area increases with the decrease in the water density
and therefore material buckling drops, whilst there is no signi-
ficant increase of K_∞ if the fuel element is homogenized over
100 or 90 % respectively of the transport position. However,
because of the sharp increase of the migration area, the con-
tainer multiplication factor will in any case drop with
decreasing water density. This fact was verified by complete
container calculations for the most reactive basket lattice
cell (homogenization of the fuel element over the whole trans-
port position, cell radius 5.7 cm, basket radius 22.076 cm).
The exact calculating model is given in chapter 3.3. The
results of these calculations are to be found in table 11.

Table 11

$\varrho\text{-H}_2\text{O}$	1.0	0.9	0.8
K_B	0.8980	0.8787	0.8541

Similarly, group constants for the various fuel element sizes,
as described in chapter 4.1, were calculated with water densi-
ties of 0.9 and 0.8 g $\cdot$ cm^{-3}. The uranium content in the core
was 21 %. The characteristic criticality measurements from
these calculations are given in table 12. It can be seen from
table 12 that the reactivity rates for the MERLIN fuel elements
are similar to those for the DIDO fuel elements (table 9).
Consequently, no calculations were made for group constants for
MERLIN basket lattice cells with reduced water densities. When
comparing a MERLIN basket lattice cell with the most reactive
DIDO basket lattice cell (without external water layer), then
the proportion of steel is 30 % higher for a MERLIN basket
lattice cell than for a DIDI basket lattice cell. As a result,

the reactivity absorption for MERLIN basket lattice cells is greater with reduced water density.

Table 12

BE.-WEITE	ϱ-H_2O	K_∞	B_m^2	τ	L^2	M^2
6.3x3.76	1.0	1.7743	.0067	111.68	4.092	115.77
	0.9	1.7631	.0058	127.46	4.573	132.03
	0.8	1.7499	.0049	147.28	4.925	152.20
6.3x7.52	1.0	1.8091	.0171	43.626	2.304	45.930
	0.9	1.8169	.0146	51.891	2.646	54.537
	0.8	1.8236	.0122	62.815	3.090	65.905
7.56x7.56	1.0	1.7791	.0182	39.289	2.304	41.593
	0.9	1.7918	.0155	47.039	2.648	49.687
	0.8	1.8037	.0129	57.363	3.094	60.457
7.96x7.96	1.0	1.7584	.0184	37.515	2.335	39.850
	0.9	1.7738	.0157	45.050	2.684	47.734
	0.8	1.7886	.0131	55.135	3.136	58.271
8.7x8.1	1.0	1.7343	.0185	36.003	2.385	38.388
	0.9	1.7525	.0158	43.355	2.742	46.097
	0.8	1.7703	.0132	53.236	3.204	56.440

7. Dry container

When investigating the criticality safety of the dry container only the MERLIN fuel elements need be taken into consideration as these have the highest fissile material content. In all, 18.56 kg U-235 can be found in the TN-7 with four fully laden inserts. The volume percent of fissile material in the active part of a fuel plate amounts to ca. 0.015. The critical, un-reflected spherical mass of U-235 at such a dilution in aluminium is ca. 1400 kg U-235 (Lit. 4), so that no criticality problem is to be expected for the dry container.

Because of the container reflection on the one hand and a neutron interaction with other containers on the other hand, two Monte-Carlo calculations were performed for an infinite expanse of square lattices composed of containers lying close together. For this the radial container structure was retained and infinite extent in an axial direction assumed. In case 1, the active part of the fuel plates was compacted to a cylinder in coaxial location (R = 9.47 cm). In case 2, it was assumed to be homogeneously distributed over the container interior. The actual basket material was always disregarded. In both cases a multiplication factor of ca. 0.51 resulted for the arrangement, so that even in a dry state any container arrangement is critically safe. This result was also to be expected from the experiments described in chapter 6.

8.0   Appendix

8.1   Container TN-7

8.2   DIDO fuel element

8.3   DIDO fuel plates

8.4   DIDO fuel element rods during transport

8.5   MERLIN fuel element cross-section

8.6   MERLIN fuel element, inner fuel plate

8.7   MERLIN fuel element, outer fuel plate

9. References

/1/ Criticality study of transport containers for irradiated
    fuel elements of the light water type
    TN, Sept. 74, H. Krug

/2/ Criticality safety of a "Dry transport container" for
    irradiated fuel elements of the light water type,
    depending on the enrichment
    TN, April 75, H. Krug

/3/ Los Alamos Group-Averaged Cross-Sections
    LAMS-2941, Hansen, Roach et al.

/4/ Handbook of Nuclear Safety
    DP-532, Jan. 61, H.K. Clark

/5/ GAMTEC II : A Code for Generating Consistent Multigroup
    Constants Utilized in Diffusion and Transport Theory
    Calculations
    BNWL - 35, March 1965
    Carter, Richey, Hughey

/6/ Nuclear Reactor Core Analysis Code : CITATION
    ORNL - TM - 2496, Rev. 2, 1971
    Fowler, Vondy, Cunningham

/7/ KENO - A Multigroup Monte Carlo Criticality Program
      CTC - 5, September 1969

10. Supplement

10.1 Boron steel basket for DIDO fuel elements

As an alternative solution to the DIDO insert described
above, another variant is considered here for which the
transport positions are out of boron steel rods. The
rod wall thickness is 0.3 cm and the boron content of the
steel is 0.6 weight percent. The internal diameter was
retained (10.4 cm). Otherwise the conditions were the
same as described in chapter 3.

Analogous with the illustration in chapter 3.2, group
constants were calculated for the new basket lattice cells.
The characteristic criticality values in table 10.1,
corresponding to table 2, were collated from this calcula-
tion.

Table 10.1

% Vol.	R_{BE}	R_{H2O}	K_∞	B_m^2	τ	L^2
100	5.2	0.0	0.8973	-.00293	33.289	1.711
90	4.9332	0.2668	0.9090	-.00260	33.309	1.684
80	4.6510	0.5490	0.9063	-.00267	33.397	1.660
70	4.3506	0.8494	0.8899	-.00314	33.458	1.647
65	4.1924	1.0076	0.8765	-.00369	33.501	1.643
60	4.0279	1.1721	0.8594	-.00399	33.556	1.648
55	3.8564	1.3436	0.8386	-.00457	33.627	1.659
50	3.6770	1.5230	0.8136	-.00527	33.717	1.681
40	3.2888	1.9110	0.7496	-.00700	33.990	1.765

In comparison with table 2, it can be seen immediately from table 10.1 that the K_∞-values alone for all basket lattice cells are under 1. In addition, the container calculations indicated above, as well as the reactivity effects can be attributed in their order of magnitude to the present case. Consequently this boron steel basket can be considered as critically safe for the transport of DIDI fuel elements in the TN-7.

10.2 Boron steel basket for MERLIN fuel elements

The boron steel basket for the MERLIN fuel elements is once again formed of almost square steel boxes with an surface of 8.7 x 8.1 cm^2. These steel boxes differ from the non-poisoned insert boxes in so far as they have a wall thickness of 0.3 cm and a boron content of 0.6 %. For the rest the same conditions as in 4.2 prevail.

Analogous with figure 4, group constants for the cases illustrated in this figure were calculated. The charac-teristic criticality values are given in table 10.2.

Table 10.2

BE	6.3x3.76	6.3x7.52	7.56x7.96	7.96x7.96	8.7x8.1
K_∞	0.6686 (0.6544)	0.9514 (0.9359)	1.0003	1.0145	1.0184
M^2	42.960 (43.090)	39.784 (39.873)	39.534	39.412	39.335
B_m^2	-.0077 (-.0080)	-.0012 (-.0016)	$7.6 \cdot 10^{-6}$	.0004	.0005

When the values in table 10.2 are compared with those
given in figure 4 it can be concluded that - on the one
hand - the reactivity of the boron-poisoned lattice is much
lower and that - on the other hand - the similar tendencies
can be detected for the reactivity effects. As a result
the multiplication factor for the TN-7 with an insert of
these boron steel boxes will be much lower than inserts of
unpoisoned steel as used in the experiments.

Appendix 8.2

Criticality safety of irradiated
RHF fuel elements in the TN 7
transport flask

W. Weber, H. Krug, 27.4.1982

Criticality safety of irradiated RHF fuel elements in the TN 7
transport flask

W. Weber, H. Krug, 27.4.1982

1. PROBLEM DEFINITION

It is intended to transport 2 irradiated fuel elements from the
high flux reactor in Grenoble (RHF fuel elements) in the TN 7
transport flask. For this purpose the transport flask must
satisfy the requirements for the nuclear fissile class II, i.e.
at least 2 flasks in a flooded, fully reflective state, and 5
flasks in a dry state are sufficiently sub-critical.

For transport, the RHF fuel elements will be sufficiently dis-
assembled such that only the cylindrical active zone is trans-
ported (drawing no. Re 7C 65 R10, Institut Max von Laue – Paul
Langevin). Both RHF fuel elements will be fixed in position
inside the transport flask by means of a basket. Inside the
transport flask itself there is also an additional shielding
unit (drawing no. 1-150- 025-19-00, TN).

Although sub-criticality in the dry state can be proven by means
of the available literature, a criticality analysis was necessary
for the flooded state.

2. FLOODED FLASKS

2.1 Method of calculation

The multiplication factor for the flooded flasks was calculated
using the Monte Carlo program KENO-IV (Lit. 1), with 15 fast and
1 thermal neutron groups. The effective cross-sections in P_1-
approximation were produced using the GAMTEC program (Lit. 2),
whereby for the fast groups a B_1-approximation and for the

thermal group with water moderation the Wigner-Wilkins approximation
was used, in other cases a Maxwell spectrum at ambient temperature.
In order to calculate the effective cross-sections of the fuel zone,
the aluminium fuel plates were homogenised with water over the
volume (formed from 6.19 cm annular gap between the aluminium load
tubes and the active height of 80 cm).   As a buckling constant,
10^{-4} was used.

2.2   Material data

Fuel isotopic composition: 9.2   kg U-235 $\rho = 18.662$ g cm^{-3}

(active zone)   17.086 kg Al $\rho = 2.698$ g cm^{-3}

Steel composition: DIN 1.4301 $\rho = 7.566$ g cm^{-3}

Densities: Aluminium $\rho = 2.698$ g cm^{-3}

                                  Lead $\rho = 10.77$ g cm^{-3}

                                  Water $\rho = 1.00$ g cm^{-3}

2.3   Geometrical model

In the calculation model, the ring-formed structure of the cross-
section through the flask at the active zone level was reproduced
in a lateral direction, whilst in the longitudinal direction a
conservatively infinite length was assumed.   Material zones and
ring thicknesses (ΔR) are listed from inside to outside in the
following table:

Zone	Material	ΔR (cm)	Component
1	water	11.20	
2	steel	0.80	basket
3	water	1.04	
4	aluminium	0.65	fuel element
5	fuel	6.19	fuel element
6	aluminium	0.80	fuel element
7	water	6.32	
8	steel	1.00	additional shielding
9	lead	5.20	additional shielding

10	steel	1.20	additional shielding
11	water	1.10	
12	steel	1.00	flask
13	lead	13.00	flask
14	insulation	3.00	flask
15	steel	2.00	flask

All empty spaces were, as you can see, completely filled with
water. Instead of the insulation (zone 14) a vacuum was assumed,
which in the present case is of minor importance for the criticality

For the Monte Carlo calculation, 2 flasks were represented touching
side to side. In addition, these flasks were assumed to be
surrounded by at least a 30 cm thick layer of water.

2.4 Result

The Monte Carlo calculation was programmed for 63 iterations, each
with 300 neutrons, whereby the first 3 iterations were devoted to
determining the multiplication factor. For the given sequence the
result was:

$$K = 0.933 \pm 0.006 \qquad \text{(accurate to 1 } \sigma)$$

Thus, 2 touching flasks when fully flooded and water reflected are
sufficiently sub-critical.

3. DRY FLASKS

There are no criticality problems for the flasks in a dry state.
This can be shown by the following estimation. Assuming 9.2 kg
U-235 and 17 kg aluminium for the fuel zone of an RHF fuel element,
then in the fully compacted fuel mass the weight percent of U-235
is 35 % and the percentage volume of U-235 is 7.3 %. According
to Lit. 3, Fig. 2.8, the critical though unreflected spherical
mass at this concentration is about 1100 kg U-235.

The influence of a reflector can also be obtained by estimation
(according to Lit. 3) by multiplying this unreflected mass by the
relation of fully-concentrated reflected to unreflected spherical

masses.   The experimental spherical masses of U(93) metal with no
reflector is 49.3 kg (according to Lit. 4), and of U(93.5) metal
with a 20 cm thick natural uranium reflector is 16.1 kg according
to Lit. 5.   Thus, the critical mass would be 359 kg.

The U-235 content of 5 transport flasks is 92 kg, which means that
at least 5 transport flasks in a dry state are sufficiently sub-
critical.   The estimation carried out is very conservative, as
the fuel zone is always assumed to be fully compacted.   Bearing
in mind the actual circumstances, it can be expected that even an
infinite number of such flasks in a dry state are sub-critical, as
detailled calculations with similar fuel have shown (see Lit. 6).

4.   REFERENCES

/1/   L. M. Petrie et al.:
       KENO-IV, An improved Monte Carlo criticality program
       ORNL-4938, Nov. 1975

/2/   Carter, Richey, Hughey
       GAMTEC-II, A code for generating consistent multigroup
       constants utilised in diffusion and transport theory
       calculations
       BNWL-35, March 1965

/3/   H.K. Clark
       Handbook of nuclear safety
       DP-532, Jan. 61

/4/   J. H. Chalmers et al.:
       Handbook of criticality data, vol. 1
       1967

/5/   H. C. Paxton et al.:
       Critical dimensions of systems containing ^{235}U, ^{239}Pu, ^{233}U
       TID 7028, June 1964

/6/   H. Krug
       Criticality safety of DIDO and MERLIN fuel elements in the
       TN 7
       Dec. 1976

9.   Quality assurance

9.1   Quality assurance manual

Quality assurance requirements are described in the TRANSNUKLEAR (TN) quality assurance manual /9-1/.

The contents of the manual are:

- Tasks and fields of application of the quality assurance system
- Organisation of the hierarchy and administration of TN including organisational charts, quality system and qualifications
- Purchasing in accordance with quality assurance requirements
- Quality assurance co-operation with suppliers
- Design and planning including development, calculations and design
- Inspection and revision of calculation, design, fabrication and testing documents as well as their release.
- Fabrication supervision and carrying out of tests and inspections
- Transport and storage
- Installation and commissioning
- Documentation including control and revision of documents
- Identification, archiving, traceability

The quality assurance manual applies to the areas of organisation, planning, fabrication, inspection and operation of the cask.

9.2 Fabrication and inspection

9.2.1 Generalities

The fabrication of the cask from its components is carried out in accordance with fabrication follow-up plans (FPP) determined by TN and the manufacturer and approved of by independent experts prior to the start of fabrication.

The manufacturer records the individual fabrication and inspection steps.

The independent expert and/or TN will inspect the progress of fabrication and the results of tests carried out at predetermined intervals.

The manufacturer follows up fabrication and inspection documentation and submits it to TN for inclusion in the overall documentation following comple-tion of the individual cask components after approval by the independent ex-pert, TN and the manufacturer.

9.2.2 Selection of manufacturer

Prior to the placing of an order, TN will investigate whether the manufactu-rers invited to tender fulfil the following quality assurance requirements:

- Organisational structure of the manufacturer
  - Organisational charts and structuring
  - Quality assurance system
    - Independent quality assurance department (with direct access to company management)
  - A quality assurance department independent of manufacturing
  - Control of quality assurance measures
    - Control of drawings/parts lists, inspection plans, welding plans
    - Material deliveries

- Welding supervision

- Inspection supervision

- Stamp control and re-stamping

- Gauging

- Licences in accordance with technical regulations

- Staff qualifications

- Determination of the quality assurance system

- Availability of one or more quality assurance manuals

- Availability of a quality assurance program or quality assurance specifications

- Testing and inspection prior to the start of fabrication

- Examination of the fabrication sites, machines and products as regards cleanliness

- Verification that all employed welders have valid professional certifications

- Proof of valid process inspections in accordance with AD specifications

- Materials

- Material reception examinations

- Identification and marking examination (stamping)

- Assignability of the material records

- Inspection and archiving of material records

- Storage of semifinished materials and welding additives

- Testing and inspection during fabrication

- Recording of fabrication and inspection steps

- Carrying out of intermediary inspections in accordance with written instructions

- Deviations as regards inspection methods and their recording

- Nonconformances in relation to fabrication methods and their recording

- Carrying out and recording of repair measures

- Welding controls
  - Control by the welding supervisor
  - Presentation of valid welding certificates
  - Examination of the welding data in relation to the welding plan
  - Comparison of welding additives (inspection as to confusions)
  - Examination and validity of welding methods
  - Examination of weld seam preparations
  - Carrying out and recording of repairs and corrections
  - Storage of welding additives

- Inspection of synthetic materials in accordance with specifications

- Inspection of the coat of paint in accordance with TN specifications

- Testing and inspections
  - Carrying out and recording of non-destructive testing
  - Carrying out of destructive testing
  - Storage, inspections and adjusting of testing equipment

- Documentation
  - Inspection of the documentation department
  - Organisation of documentation according to TN specifications
  - Archiving documentation

When a manufacturer is invited to tender, he is previously provided the TN order specifications and draft drawings of the cask. The final specifications will be worked out by TN in collaboration with the manufacturer, based on the order specifications.

9.2.3   TN specification TN 7-2

The specification contains the following main items:

- field of application and responsibilities
- specification changes
- design characteristics of the cask
- cask description
- handling description
- classification of components according to requirement categories
- description and specification of components
- material specifications
- submission of preliminary inspection documents
- taking into account of technical regulations and TN regulations
- materials testing
- carrying out of welds
- testing and inspection during fabrication
- testing and inspection of the finished cask (final acceptance)
- documentation
- fabrication inspection plan
- material data sheets
- fabrication follow-up plan
- inspection plans
- drawings

Specification "TN 7-2 Transport Cask for Spent Fuel Assemblies", no. 06
BBO 23 revision 3 /9-2/ thus prescribes the entire fabrication process.
Prior to fabrication, the documents are submitted to the competent autho-
rities for preliminary inspection and fabrication clearance.

9.2.4   Preliminary inspection documents

Preliminary inspection documents are:

- TN 7-2 specification
- materials data sheets
- fabrication follow-up plan
- welding plan
- fabrication blueprints and parts lists
- welding blueprints

Fabrication of the components will only begin after clearance of the pre-liminary inspection documents has been granted by the competent autho-rity.

9.2.4.1   Specification TN 7-2

Cf. chapter 9.2.3

9.2.4.2   Construction materials data sheets

The material data sheets list all the materials and standard parts used for the fabrication of the cask, corresponding data and the inspections to be carried out. Depending on the grading of the individual component the scope of inspections and the type of required verifications is determined. Material data sheets are examined by the competent authority. They are part of the specifications. Materials are selected on the base of generally accepted technical regulations.

9.2.4.3   Fabrication follow-up plan

The fabrication follow-up plan indicates inspections required prior to, during and following fabrication, based on the fabrication inspection plan. The main fabrication and inspection steps pertaining to the fabrication of the individual components are described chronologically. Implementation is confirmed, depending on the specification grading, by the manufacturer, TN and/or an independent expert.

The fabrication follow-up plan also contains references with regard to the documents it is based on, fabrication regulations to be complied with and inspection regulations.

9.2.4.4   Welding plan

The welding plan is worked out in accordance with TN specifications. It contains following information (if required):

- welding plan number
- order number
- purchaser
- subject
- number of blueprint
- designation of the welding materials
- welding method
- work samples
- preheating temperature/temperature of intermediate layers
- electrode drying
- welding data
- weld seam inspections
- sketches with running weld numbers
- weld seam preparation
- treatment of edges

- root face finishing
- weld seam sequence
- number of layers
- weld seam finishing
- acceptance

The welding plan must be cleared by the competent authority before fabrication may begin. Its requirements must be complied with.

9.2.4.5   Fabrication and welding blueprint

If necessary, fabrication and welding blueprints for all components will be submitted for preliminary inspection. In this case, fabrication blueprints also include welding blueprints with every weld seam marked in accordance with the numbering in the welding plan.

Fabrication blueprints include the corresponding parts lists.

9.2.4.6   Changes of the quality assurance plan

The quality assurance plan includes all preliminary inspection documents. It also includes specific work and inspection instructions.

Any change of the quality assurance plan resulting from preliminary inspection will cause the implementation of the following measures, depending on the requirement category:

-   For parts which fall by definition into requirement category I, changes will be reported by the manufacturer to TN, to the officially approved expert and to the competent authority. Any deviation will require the approval of the authority.

- For parts falling under requirement category II, TN and the independent expert shall be informed. Any alteration or deviation requires the latter's approval.

- For parts falling under requirement category III, TN is informed. TN's approval is required for any alteration. The official expert is informed about the alteration.

9.2.5   Special working and inspection instructions

Special working and inspection instructions are worked out by TN for some fabrication steps, or in collaboration with the manufacturer.

This particularly concerns insertion of the thermal insulation (cement). The manufacturer will investigate the behaviour of the cement during and after casting in the course of preliminary tests. The casting of cement into the 1/3 scale model, following simulation tests, will serve as a process qualification for the casting of cement into the original TN 7-2 cask.

Similarly, the painting of the outer cask surface is carried out according to TN working instructions, except for the trunnions. Requirements concerning the paint are listed in the TN specifications.

9.2.6   Destructive and non-destructive tests

The different cask components will continuously be submitted to tests during fabrication.

Where this is considered necessary, process and accompanying samples will be submitted to destructive tests. Non-destructive tests, such as ultrasonic tests, surface crack testing, gauging etc. will be carried out during fabrication.

For every component there is a material data sheet which indicates:

- the type of inspection
- the extent of testing
- verification
- tester

During fabrication, the components will be submitted to additional non-destructive tests. These tests are defined in the fabrication and test follow-up plans.

9.2.7   Acceptance

After completion and assembly of the cask, the following tests are carried out in accordance with the fabrication follow-up plan, in the presence of the appointed independent expert, of the manufacturer and of TN. Correct execution of these tests is confirmed by the independent expert:

- stamp control
- examination of the confirmed fabrication and inspection follow-up plan
- leak tests
- load tests of the handling components followed by tests of their weld seams
- gauging
- examination of documentation

The manufacturer will carry out inspections and handling tests in presence of TN. These will demonstrate that the cask and its handling components can be handled without problem. These tests comprise:

- determination of weight
- examination of the surface as to absence of ferrite

- pressure test and visual inspection of the containment
- heating test
- examination of the coat of paint
- examination of the cask markings according to TN specifications
- handling tests:
  . installation and disassembly of all lids and connections
  . attachment and removal of the trunnions
  . turning of the cask over the lower pair of trunnions
  . testing of the proper function of the cask openings
  . vacuum drying

Following the tests to be supervised by the independent expert, the cask will be stamped for release if there are no objections, and marked with the date of the next periodic inspection.

9.3   Integrated fixtures

A. Insert baskets for DIDO and MERLIN fuel assemblies

The insert baskets for DIDO and MERLIN fuel assemblies are welded stainless steel structures (cf. chapter 3)

The same insert baskets are used in the TN 7-2 cask as in the TN 7.

Additionally, a new insert basket for MERLIN fuel assemblies will be built based on the existing MERLIN basket. This new basket will be fabricated observing the usual quality assurance requirements in accordance with TN
specifications as well as fabrication and inspection follow-up plans.

B. RHF basket

The RHF basket (cf. chapter 3) is a welded stainless steel structure.

The basket will be fabricated in accordance with TN specifications and fabrication and inspection follow-up plans, observing quality assurance requirements.

9.4   TN 7-2 transport cask - 1/3 scale model

The cask model is fabricated by the same manufacturer as the original cask. Fabrication and inspection of the model are carried out in accordance with TN specifications /9-3/. These specifications are submitted for preliminary inspection together with the fabrication and welding blueprints and a welding plan. Any changes to these documents are also subject to approval as set out in chapter 9.2.4.6.

The scope of tests during the fabrication of the model is smaller than that required for the original cask; however, it will be ensured that the 1/3 scale model is representative of the original cask during tests. This will, in particular, mean that dimension relations of the model are according to the same scale, that the same or at least comparable materials are used and that the welds are comparable. For this purpose, material verifications are carried out, if possible by means of 3.1 B certificates, and a welding plan is drawn up.

Deviations occurring in the scale model are such that they either have no consequence or are conservative as far as the drop and fire tests are concerned.

9.5   Literature

/9-1/   TN Quality Assurance Manual, Revision 0
           February 1982

/9-2/   Specifications for the TN 7-2 Transport Cask for Irradiated Fuel
           Assemblies, no. 06 BBO 23 Revision 4

/9-3/   Specifications for the 1/3 Scale Model of the TN 7-2 Transport Cask for
           Irradiated Fuel Assemblies no. 06 BBO 24 Revision 2

10.   Handling and periodic inspections

The main handling steps with regard to the loading and unloading of the cask are described below inasmuch as they are safety relevant (cf. Fig. 10-1). The description will cover the various types of loading in common without taking into account differing local conditions. In addition, detailed handling instructions will be worked out for the various types of loading.

Should the cask be handled in other nuclear facilities, this will be considered in new instructions if necessary.

Carrying out of tests by the operator prior to each loading are part of the handling instructions. Periodic inspections are those tests carried out at certain time intervals, some of them in the presence of an independent expert.

10.1   Loading of cask

10.1.1   Preparations for loading

- Visual inspection of the overall condition, if necessary cleaning of the cask.
- Taking of a gas sample from the inside and analysis (only in the case of RHF fuel).
- Leak check in accordance with TN specifications prior to loading (if any leakage is discovered, the gaskets are replaced and the tests are repeated).
- Unscrewing of the cask lid screws and screwing-in of the eyebolts.
- Removal of the coupling in the cask bottom (position A) and attachment of the matching coupling in the lid (position B).

- Placing the lid centring pins in two lid screw holes.
- Removal of cask lid (in the case of RHF fuel, this operation, together with the following activities, is not carried out under water; normally this is carried out in the pond).
- Visual inspection of the lid and the cask cavity.
- Removal of the insert baskets from the cask, visual inspection of the cask cavity (particular care should be taken that no components are lying around in the cask).
- Visual inspection of the insert baskets, if necessary, a test loading with a dummy will be carried out.

10.1.2 Loading

- The cask is set down in the pond with the help of a crane. The crane attachments are removed from the cask (this will normally be done prior to the removal of the cask lid).
- The fuel assemblies are loaded into the insert baskets.
- The loaded baskets and the spacers are placed inside the cask.
- The lid is attached under water, taking particular care taken as to proper fitting.
- The cask is lifted up to the water surface and the lid is provisionally secured with three screws.
- The cask is lifted altogether out of the water and rinsed on the outside with fully demineralized water. While the cask is lifted out, the dose rate is being monitored.
- The cask is emptied of water above the pond and then placed in its predetermined position.
- Coupling A is screwed in.

10.1.3   Preparation for transport

- The lid centring bolts are unscrewed.
- The lid screws are applied and fastened with a torque of 400 Nm.
- The cask cavity is dried (vacuum drying over the bottom connection (A), with lid connection (B) closed. For this, the cavity must be evacuated to less than 20 Torr.
- Transport vacuum of 0.6 bar is adjusted.
- The drying equipment is removed and the protective lid applied over the couplings (A, B). Tightening torque of the screws: 15 Nm.
- Leak checks are carried out in accordance with TN specifications. A leak rate of $L \cong 1 \cdot 10^{-2}$ is determined for the cask. This is demonstrated by loss of pressure.
- The testing connections are closed off and the cask is sealed.
- The shock absorbers are fitted.
- The cask is decontaminated. According to traffic regulations, the maximum admissible values are:

$$\alpha : 10^{-5} \, \mu Ci/cm^2$$
$$\beta + \gamma : 10^{-4} \, \mu Ci/cm^2$$

- The cask is inspected for compliance with the traffic regulations concerning dose rate, surface temperature and contamination.

10.2   Unloading of cask

10.2.1   Preparations for unloading

- Receiving inspection of the cask:
  dose rate, temperature and contamination are checked, the overall
  condition of the cask is examined.
- The shock absorbers are removed.
- The protective lid covering the coupling (positions A and B) is removed.
- A gas sample is taken at connection A.
- The coupling is removed from connection A.
- Lid coupling (B) is connected to a hose which is closed off at the end.
- The cask is lowered into the pond and left to cool down (about 4 hours).
- Water is let through the lower opening into the cask by opening up the
  hose. The end of the hose is held under water in order to allow released
  steam to condense. The filling of the cask will take approximately one
  hour.

10.2.2   Unloading

- The cask is lifted up to the water surface, the lid screws are unfastened
  and the centring bolts are screwed in.
- The cask is lowered again.
- The cask lid is drawn under water.
- The baskets containing the fuel assemblies are unloaded from the cask.
- The empty baskets are reloaded.
- The cask is lifted from the pond and rinsed on the outside with fully de-
  mineralized water.
- The cask is emptied of water over the pond and then placed in a prede-
  termined position.

10.2.3   Preparations for transport

- The lid is applied, centring bolts are removed and screws are fastened.
- The lower coupling (A) is screwed in.
- The cask cavity is dried (vacuum drying).
- The protective lid is placed over the couplings.
- The cask is decontaminated.
- The shock absorbers are fitted.
- The cask is inspected for compliance with the traffic regulations concerning dose rate, surface temperature and contamination.

10.3   Periodic inspections

The plan for periodic inspections is contained in appendix 10.1.

Appendix 10.1

Plan for periodic inspections

Plan for periodic inspections of the TN 7-2 transport cask

These inspections are carried out by the officially approved expert. The inspection interval is set at four years.

The following inspections will have to be carried out:

1. External and internal visual inspection of the overall condition as regards corrosion and mechanical changes.

2. Visual examination of the gasket surfaces with regard to corrosion and mechanical damages.

3. Visual examination of the screws for mechanical damage.

4. Inspection of the type plate as to completeness.

5. Visual examination of the fuel assembly insert baskets with regard to corrosion and mechanical changes.

6. Surface crack inspection of the trunnions as well as of the weld seams marked in Fig. 10-1 using the dye penetration process. This is carried out and evaluated in accordance with TN inspection procedure no. 04-100-1981.

7. Leak checks of the lid gasket and the two coupling lids.
   Maximum total leak rate for the cask: 10^{-4} Torr · l/sec

   Inspection space between the double gaskets: maximum leak rate $3 \cdot 10^{-4}$ Torr · l/sec

The tests are carried out using a process which ensures that the leak rates quoted above can be detected. This may be for example helium leak test or tests of pressure increase test or drop of pressure.

11.   Drawings

The following drawings are joined to the safety report. They are referred
to in the text:

- Overview   No. 0-150-050-04-00

- Cask body   No. 0-150-050-05-00

- Cask lid   No. 0-150-050-06-00

- Lid shock absorber   No. 1-150-050-07-00

- Bottom shock absorber   No. 1-150-050-08-00

- Type plate   No. 3-150-050-03-00

- Insert baskets for MERLIN and
  DIDO fuel assemblies   No. 1-150-025-17-00

- Insert basket for 2 RHF fuel assemblies   No. 1-150-025-21-00

Appendix 8.1

Criticality safety of DIDO and
MERLIN fuel assemblies in the TN 7 cask

(H. Krug, Technische Universität München,
December 1976)

Ref.: TN 7-2 _____Drawing no: 0-150-050-04-00

Explanations:

TN - TRANSNUKLEAR

 T - officially approved
       expert

Part 2:

Test after 4 years

No	Description of inspection	Inspection procedure	Inspector	
			TN	T
	step			
1	Inspections according to Part 1, no. 1, 2 and 5		x	
2	Exterior and interior inspection of overall conditions for corrosion and mechanical changes	visual		x
3	Inspection of gasket surfaces for corrosion and mechanical changes	visual, rework if necessary		x
4	Surface crack inspection of lid and protective lid screws	TN inspection procedure no. 04-100-1981		x
5	Control of all threads as to easy going	Working procedure, rework if necessary		x
6	Removal of trunnions, surface crack inspection of parts which are not accessible from outside, surface crack inspection of trunnion screws	TN inspection procedure no. 04-100-1981		x
7	Check of trunnion load with 125 % load, followed by surface crack inspection	TN inspection procedure Working procedure no. 04-100-1981		x
8	Surface crack inspection of the weld seams of the trunnion holders and the connecting seams of the exterior mantle with the bottom and the covering plate	TN inspection procedure no. 04-100-1981		x
9	Inspection of the insert baskets or corrosion and mechanical changes	visual		x
10	Inspection of the cask cavity for corrosion and mechanical changes	visual	x	
11	Helium leak check at gaskets of lid and protective lid	TN inspection procedure no. 04-110-1982		x
12	Inspection of shock absorbers for tightness	TN inspection procedure, gas pressure 1.1 bar, soap bubble test	x	
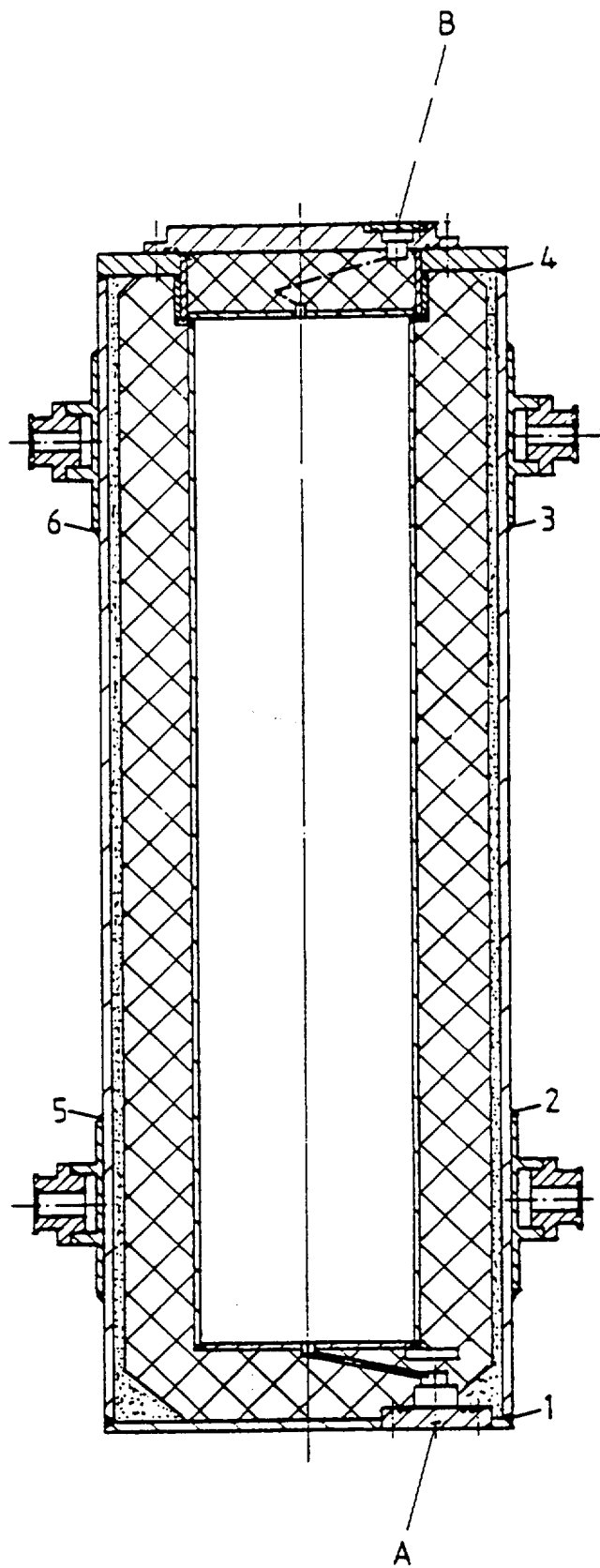
(1 - 6 subject to periodic inspections)
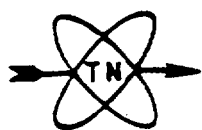
Transport cask TN 7-2

Fig. 10-1

Partial Translation of letter schi/rl-7 concerning criticality

Certificate D/4160/B(U)F-85 (Rev. 3)
Your letter ET 3.2-D/4160-Sr/Ts of 29.11.94

Dear Sirs,

Herewith we apply for incorporation of MTR fuel elements type SAPHIR under content 1b) of above certificate. These elements essentially correspond to the type MERLIN (see our letter of 25.11.94).

Possible effects on reactivity of MERLIN fuel elements caused by different nuclide densities were investigated and covered in /1/ regarding concentration of Uranium between 21 and 30 %. Therefore a new criticality safety study is not necessary.

/1/   Criticality safety of DIDO- and MERLIN fuel elements
          in the TN 7 (H. Krug, Technical University of Munich,
          December 1976)

Translation of letter schi/rl-91

Certificate D/4160/B(U)F-85 (Rev. 3)

Dear Dr. Schweer,

In the packaging TN 7/2 irradiated MTR-fuel elements of type SAPHIR should be carried. These elements correspond to the elements of type MERLIN except of insignificant differences having no influence on criticality safety.

A comparison shows the following table:

	MERLIN	SAPHIR
Active cross section	4901 mm²	4908 mm²
Thickness of plates	1.27 mm	1.27 mm
Distance between plates	2.15 mm	2.23 mm
Number of plates	23	23
U/Al	27 %	27 %
Active length	600 mm	600 mm

All other conditions concerning quantities, enrichment, decay time, activity and decay heat were observed.

Please inform us as soon as possible if the elements of type SAPHIR can be carried under content 1 b) of above certificate or if a modification of the certificate is necessary.